Introducing (Inter-)Halogen Polysulfates – A Study on the Influence of Halogen Bonding on Weakly Coordinating Anions

Jan Langwald,[a] Rosa M. Gomila,[b] David van Gerven,[a] Antonio Frontera,[*b] and Mathias S. Wickleder[*a]

Table of Contents

[a] Institute of Inorganic and Materials Chemistry, University of Cologne, Greinstr. 6, 50939 Cologne, Germany.
E-mail: mathias.wickleder@uni-koeln.de
[b] Universitat de les Illes Balears, Crta de Valldemossa km 7.5, 07122 Palma de Mallorca, Baleares, Spain.
E-mail: toni.frontera@uib.es

A. Synthesis

General Procedure

SO_3 was obtained in a specially designed apparatus for the generation, distillation and the subsequent transfer into glass ampoules under nitrogen gas. For this purpose, fuming sulfuric acid (5 mL, 65% SO_3, used as received, Merck, Darmstadt, Germany) was added via a dropping funnel into a 500 mL flask with P_4O_{10} (250 g, >97%, Merck, Darmstadt) with a dosage rate of 1 mL / minute. At the same time, the flask was heated at 130 °C and the generated SO_3 distilled into a connected burette body (scaling 0.01 ml). A connected glass ampoule (*l* = 200 mm, ø = 16 mm, thickness of the tube wall = 1.80 mm) containing the solid starting materials was then filled with the required amount of SO_3.

Synthesis of $[IBr_2]_2[S_4O_{13}]$ (1)

265.9 mg (1.05 mmol, 1.00 eq.) of I_2 (Riedel-de Haën, Seelze) and 187 mg (1.17 mmol, 1.11 eq.) of Br_2 (Thermo Fischer Scientific) were filled into a oven-dried glass ampoule (3.3 borosilicate). 0.22 mL SO_3 (5.50 mmol, 5.23 eq.) were condensed on top and the ampoule was sealed under reduced pressure ($1 \cdot 10^{-3}$ mbar) with a gas burner. The reaction vessel was heated to 80 °C within 24 h, dwelled at this temperature for 48 h and cooled down to room temperature (in the following 'r.t.') within 90 h. After cooling, dark red-brown crystals grew in the mother liquid.

Synthesis of $[I_3]_4[S_4O_{13}]_2(SO_3)$ (2)

385.5 mg (1.52 mmol, 1.00 eq.) of I_2 (Riedel-de Haën, Seelze) were filled into a preheated glass ampoule (3.3 borosilicate). 0.20 mL SO_3 (5.00 mmol, 3.3 eq.) were condensed on top and the ampoule was sealed under reduced pressure ($1 \cdot 10^{-3}$ mbar) with a gas burner. The reaction vessel was heated to 80 °C within 24 h, dwelled at this temperature for 48 h and cooled down to r.t. within 90 h. After cooling, dark red crystals grew in the mother liquid.

Synthesis of $[ICl_2][HS_2O_7]$ (3)

233.0 mg (1.00 mmol, 1.00 eq.) of ICl_3 (in-house synthesis [1]) were filled into a preheated glass ampoule (3.3 borosilicate). 0.20 mL SO_3 (5.00 mmol, 5.00 eq.) were condensed on top and the ampoule was sealed under reduced pressure ($1 \cdot 10^{-3}$ mbar) with a gas burner. The reaction vessel was heated to 80 °C within 24 h, dwelled at this temperature for 48 h and cooled down to r.t. within 90 h. After cooling, an orange liquid was received. Upon placing a droplet of the liquid on a microscope slide, yellow platelets grew in the mother liquid within 5 minutes.

Synthesis of $[ICl_2]_2[S_2O_7]$ (4)

233.0 mg (1.00 mmol, 1.00 eq.) of ICl_3 (in-house synthesis [1]) were filled into a preheated glass ampoule (3.3 borosilicate). 0.25 mL SO_3 (6.25 mmol, 6.25 eq.) were condensed on top and the ampoule was sealed under reduced pressure ($1 \cdot 10^{-3}$ mbar) with a gas burner. The reaction vessel was heated to 80 °C within 24 h, dwelled at this temperature for 48 h and cooled down to r.t. within 90 h, yielding an orange solution. After cooling down to –20 °C, crystalline orange needles grew from the solution.

Synthesis of $Li_2[S_4O_{13}]$ (5)

144 mg (5.50 mmol, 1.00 eq.) of Bis(trifluoromethane)sulfonimide lithium salt $LiNTf_2$ (Sigma-Aldrich) were filled into a preheated glass ampoule (3.3 borosilicate). 0.70 mL SO_3 (17.49 mmol, 34.83 eq.) were condensed on top and the ampoule was sealed under reduced pressure ($1 \cdot 10^{-3}$ mbar) with a gas burner. The reaction vessel was heated to 100 °C within 24 h, dwelled at this temperature for 48 h and cooled down to r.t. within 90 h. After cooling, colorless crystals grew from the bulk phase.

Proposed Reactions Equations

In order to synthesize the (inter-)halogen compounds, we started from our previously reported method for the generation of $[I_4][S_6O_{19}]$,[2] and decreased the amount of SO_3 towards nearly stochiometric amounts. We suggest that this leads to an increased probability of gas-phase reactions compared to the usual solvothermal procedure where SO_3 acts as a solvent and reactant for the reaction.

While we found nearly complete conversion SO_3 with a mixture of I_2 and Br_2 towards a dark-red crystalline solid $[IBr_2]_2[S_4O_{13}]$ (**1**), we received a dark blue and bright orange solution in case of the reaction of SO_3 with I_2 and ICl_3, respectively. Subsequent storage at 7 °C led to crystallization of dark blue-purple $[I_3]_4[S_4O_{13}]_2(SO_3)$ (**2**).

When ICl_3 was used, we received bright orange solutions. Upon placing the orange solution on a microscope slide at ambient atmosphere, light yellow crystals of $[ICl_2][HS_2O_7]$ (**3**) grew. We therefore suggest that a hydrolysis by the moisture from the ambient atmosphere towards the hydrogendisulfate took place. When the orange solution was stored at –20°C, bright orange crystals of $[ICl_2]_2[S_2O_7]$ (**4**) grew.

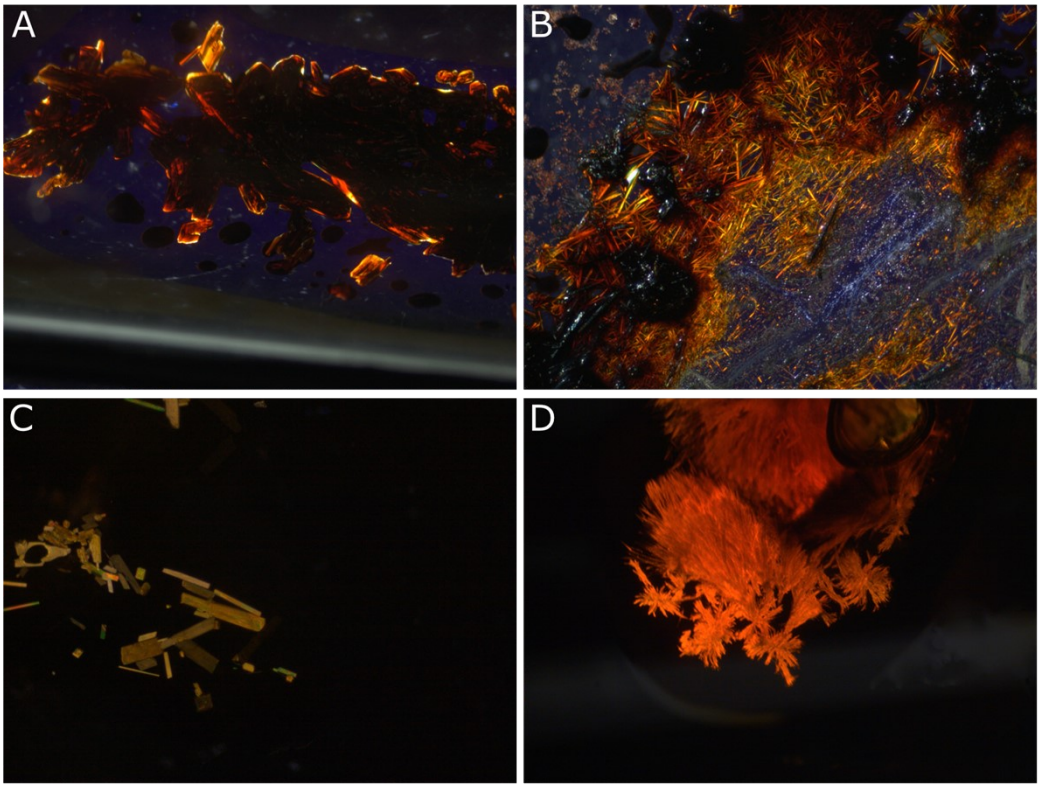

Figure S1: Crystal pictures of $[IBr_2]_2[S_4O_{13}]$ (A), $[I_3]_4[S_4O_{13}]_2(SO_3)$ (B), $[ICl_2][HS_2O_7]$ (C) and from the surrounding matrix from which $[ICl_2]_2[S_2O_7]$ was isolated (D). The pictures were taken using a light microscope with an equipped polarization filter.

We attribute these differences to the different complexity of ionic environment in the respective systems. Gillespie et al. were already able to investigate the presence of $[I_n]^+$ (n = 2, 3) in oleum conductometrically and spectroscopically and proposed that $[I_5]^+$ is present as well.[3, 4] Since our group was able to show that $[I_4]^{2+}$ is also available from the mixture I_2/SO_3, this leads to at least four different cations and several possible anions. For ICl_3, the equilibrium between $[ICl_2]^+$ and $[ICl_4]^-$ in solution is well-known and was used for the preparation of $[ICl_2]^+$ compounds before.[5, 6]

Thus, we suggest that the more complex ionic systems I_2/SO_3 as well as ICl_3/SO_3 lead to the formation of ionic liquids after the reaction with SO_3, which is why crystallization at reduced temperatures is necessary.

Based on these findings we propose the in Fig. S2. shown reaction equations. We were not able to further analyze the reactions mixtures via GC/MS yet to verify the formation of the gaseous byproducts.

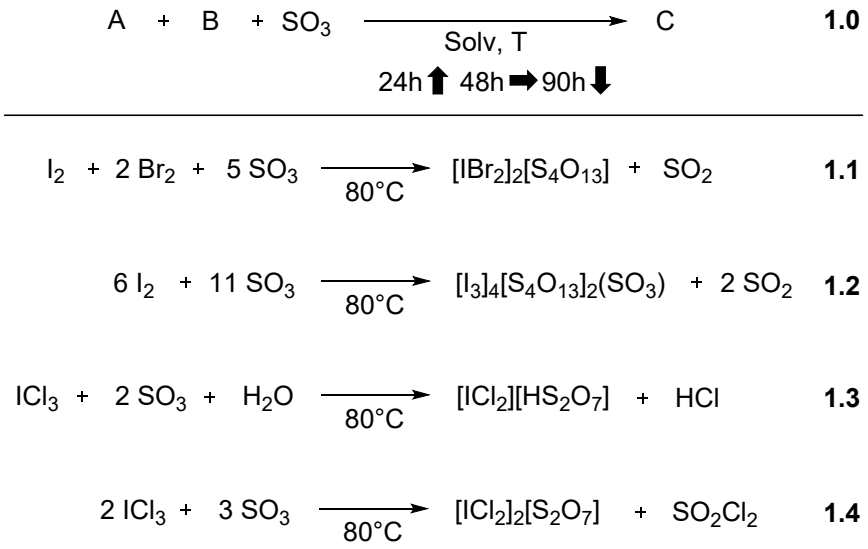

Figure S2: Generalized reaction equation (1.0) and proposed reaction equations for the formation of products 1 to 4 (1.1 to 1.4), respectively. All reactions were carried out in borosilicate glass ampules. The in eq. 1.0 given times represent the duration of heating, dwelling and cooling to room temperature.

B. Structure Determination and Crystallographic Details

General Procedure

The single crystal structure determination was performed on a *Bruker D8 VENTURE KAPPA* diffractometer with a microfocus sealed tube using a multilayer mirror as the monochromator and a *Bruker PHOTON III* detector. As characteristic X-ray radiation MoK_α (λ = 71.073 pm) or AgK_α (λ = 56.086 pm) was used for the measurements. Before the measurements, the crystals were prepared in perfluorinated ether oil (Fomblin® YR-180) and selected using a light microscope with equipped polarization filter. A suitable single crystal was fixed on a MiTeGen micromount (150 µm polymer loop) and adjusted to the X-ray beam and cooled down to 100 K in a stream of N_2. The images with the intensity data were processed using the software *APEX5*.[7] The frames were integrated with the Bruker *SAINT* software package using a narrow frame algorithm. Absorption effects were corrected using SADABS for the multi-scan absorption correction.[8, 9] The structure solution and refinement were done with the software *OLEX2*.[10] Dual methods using *SHELXT* were used for structure solution and full-matrix least-squares methods against F^2 using *SHELXL* for the refinement.[11, 12] All illustrations of the crystal structures were made with the program *Diamond 4* using the .cif as the input file.[13]

$[IBr_2]_2[S_4O_{13}]$

Table S1: Crystallographic data of $[IBr_2]_2[S_4O_{13}]$.

Empirical formula	$Br_4I_2O_{13}S_4$
Formula weight	909.68 g/mol
Temperature	100.00 K
Crystal system	triclinic
Space group	$P\bar{1}$ (No. 2)
Unit cell dimensions	a = 991.63(5) pm b = 1059.74(6) pm c = 1076.89(6) pm α = 66.868(2)° β = 72.951(2)° γ = 63.040(2)°
Volume	918.40(9) Å^3
Z	2
ρ_{calc}	3.290 g/cm^3
μ	6.684 mm^{-1}
F(000)	828
Crystal size	0.67 × 0.38 × 0.24 mm^3
Radiation	AgK_α (λ = 0.56086 nm)
2Θ range for data collection	4.046 to 51.232
Index ranges	-15 ≤ h ≤ 15, -16 ≤ k ≤ 16, -16 ≤ l ≤ 16
Reflections collected	72400
Independent reflections	7030 [R_{int} = 0.0590, R_σ = 0.0289]
Completeness to Θ = 39.3°	99.7%
Absorption correction	multiscan
Min. and max. transmission	0.234 / 0.745
Data/restraints/parameters	7030/0/209
Goodness-of-fit on F^2	1.033
Final R indexes [I>=2σ (I)]	R_1 = 0.0333, wR_2 = 0.0876
Final R indexes [all data]	R_1 = 0.0366, wR_2 = 0.0905
Largest diff. peak/hole	3.04/–1.69 e · Å^{-3}
CCDC-No.	2405908

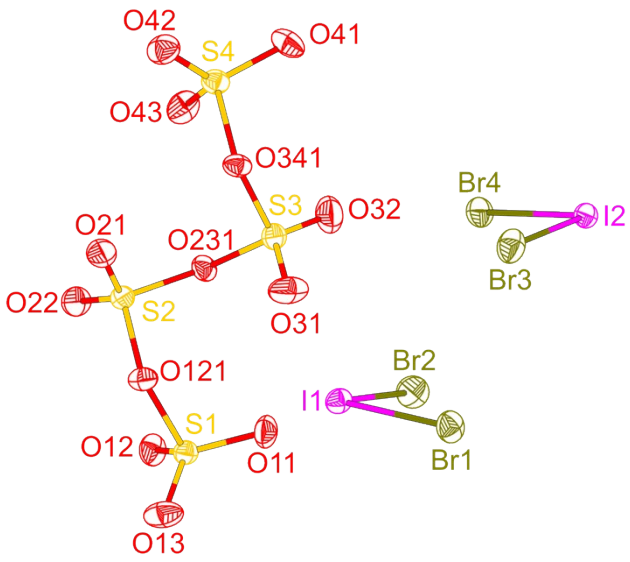

Figure S3: ORTEP of the asymmetric unit of $[IBr_2]_2[S_4O_{13}]$. Thermal ellipsoids shown with 70% probability.

Table S2: Fractional Atomic Coordinates (×10⁴) and Equivalent Isotropic Displacement Parameters (Å²×10³) for $[IBr_2]_2[S_4O_{13}]$. U_{eq} is defined as 1/3 of the trace of the orthogonalised U_{IJ} tensor.

Atom	*x*	*y*	*z*	U(eq)
I1	4221.4(3)	6904.1(2)	1426.8(2)	13.73(6)
Br1	3374.9(4)	9571.6(4)	156.7(4)	18.15(8)
Br2	1981.0(4)	6542.0(4)	1182.5(4)	18.11(8)
I2	–613.2(2)	11891.5(2)	2660.1(2)	12.57(6)
Br3	1788.3(4)	12155.4(4)	2565.2(4)	18.13(8)
Br4	266.6(4)	9161.3(4)	3537.5(4)	18.10(8)
S1	8215.9(10)	6202.2(9)	1512.2(8)	12.58(14)
S2	7935.6(10)	5571.3(10)	4458.7(9)	14.90(15)
S3	5159.6(11)	8167.6(10)	4389.0(9)	16.05(15)
S4	4613.7(10)	7316.5(10)	7323.1(9)	14.48(15)
O121	8616(3)	6203(3)	2955(3)	15.4(5)
O11	6775(3)	7445(3)	1295(3)	19.5(5)
O12	8107(3)	4798(3)	1853(3)	17.5(5)
O13	9527(4)	6403(4)	605(3)	23.0(6)
O231	6119(3)	6440(3)	4407(3)	14.3(4)
O22	8371(3)	6055(4)	5271(3)	22.6(6)
O21	8165(4)	4069(3)	4776(3)	23.8(6)
O341	5410(3)	8140(3)	5762(3)	14.2(4)
O31	3652(4)	8370(4)	4416(3)	25.9(6)
O32	5893(4)	9045(3)	3353(3)	27.2(7)
O41	3062(3)	8362(4)	7454(3)	21.0(5)
O42	5568(3)	7203(4)	8158(3)	20.7(5)
O43	4777(4)	5944(3)	7204(3)	19.9(5)

Table S3: Anisotropic Displacement Parameters (Å²×10³) for $[IBr_2]_2[S_4O_{13}]$. The anisotropic displacement factor exponent takes the form: $-2\pi^2[h^2a^{*2}U_{11}+2hka^*b^*U_{12}+\ldots]$.

Atom	U_{11}	U_{22}	U_{33}	U_{23}	U_{13}	U_{12}
I1	16.61(10)	11.85(10)	12.67(9)	–2.73(7)	–1.48(7)	–6.61(8)
Br1	18.59(16)	12.46(15)	20.43(16)	–2.60(12)	–2.83(12)	–5.49(12)
Br2	19.92(16)	14.45(15)	17.89(15)	–2.33(12)	–0.52(12)	–8.38(12)
I2	13.54(10)	10.19(10)	12.81(9)	–2.73(7)	–1.52(7)	–4.46(7)
Br3	20.24(16)	15.62(15)	19.69(16)	–5.07(12)	–8.56(12)	–4.65(12)
Br4	19.92(16)	11.04(14)	18.69(16)	–3.89(11)	–2.25(12)	–2.93(12)
S1	13.7(3)	11.3(3)	12.0(3)	–3.3(3)	–1.2(3)	–4.8(3)
S2	17.0(4)	12.0(3)	11.5(3)	–3.9(3)	–2.1(3)	–1.8(3)
S3	19.3(4)	9.7(3)	14.3(3)	–3.1(3)	–2.3(3)	–2.1(3)
S4	14.9(4)	14.8(4)	13.6(3)	–4.1(3)	0.8(3)	–7.5(3)
O11	21.3(13)	12.9(12)	20.5(12)	–4.0(9)	–8.8(10)	–0.7(10)
O12	20.8(12)	10.7(11)	21.2(12)	–5.0(9)	–6.2(10)	–4.0(9)
O13	24.0(14)	35.2(17)	15.0(12)	–7.5(11)	3.9(10)	–19.9(13)
O21	20.2(13)	28.0(15)	18.5(12)	–12.6(11)	–5.5(10)	–2.2(11)
O22	32.0(16)	9.4(11)	17.9(12)	–2.5(9)	–1.3(11)	–0.5(10)
O31	44.9(19)	13.1(12)	16.2(12)	–3.7(10)	4.5(12)	–11.1(12)
O32	20.2(14)	25.5(15)	29.1(15)	–10.5(12)	–10.3(11)	–0.3(11)
O41	13.6(11)	25.5(14)	23.8(13)	–12.1(11)	3.6(10)	–7.5(10)
O42	21.0(13)	26.4(14)	17.5(12)	–6.9(10)	–3.5(10)	–10.6(11)
O43	26.8(14)	13.8(12)	19.6(12)	–1.0(9)	–4.2(10)	–11.3(10)
O121	17.0(11)	19.0(12)	11.7(10)	–6.1(9)	–0.2(8)	–8.0(9)
O231	14.3(11)	10.2(10)	16.5(11)	–4.5(8)	–1.0(8)	–3.5(8)
O341	16.8(11)	13.0(11)	12.1(10)	–4.3(8)	2.1(8)	–7.3(9)

Table S4: Bond Lengths for $[IBr_2]_2[S_4O_{13}]$.

Atom	Atom	Length/pm	Atom	Atom	Length/pm
I1	Br1	245.97(4)	S2	O22	141.0(3)
I1	Br2	251.93(4)	S2	O21	141.2(3)
I2	Br3	248.97(4)	S3	O231	163.2(3)
I2	Br4	246.41(4)	S3	O341	155.6(3)
S1	O121	171.3(3)	S3	O31	140.4(3)
S1	O11	144.2(3)	S3	O32	140.0(3)
S1	O12	143.3(3)	S4	O341	170.5(3)
S1	O13	142.6(3)	S4	O41	143.7(3)
S2	O121	156.3(3)	S4	O42	142.5(3)
S2	O231	161.6(3)	S4	O43	144.2(3)

Table S5: Bond Angles for $[IBr_2]_2[S_4O_{13}]$.

Atom	Atom	Atom	Angle/°	Atom	Atom	Atom	Angle/°
Br1	I1	Br2	96.409(15)	O31	S3	O231	108.71(17)
Br4	I2	Br3	99.264(15)	O31	S3	O341	106.38(18)
O11	S1	O121	103.26(15)	O32	S3	O231	102.60(18)
O12	S1	O11	113.12(18)	O32	S3	O341	111.83(18)
O12	S1	O121	105.51(15)	O341	S3	O231	102.52(14)
O13	S1	O11	116.42(19)	O41	S4	O43	114.35(18)
O13	S1	O12	117.11(19)	O41	S4	O341	103.92(16)
O13	S1	O121	98.37(16)	O42	S4	O41	115.64(18)
O21	S2	O22	122.0(2)	O42	S4	O43	116.62(18)
O21	S2	O121	106.41(18)	O42	S4	O341	99.70(16)
O21	S2	O231	109.41(16)	O43	S4	O341	103.53(15)
O22	S2	O121	111.87(17)	S2	O121	S1	126.70(17)
O22	S2	O231	103.28(18)	S2	O231	S3	124.30(17)
O121	S2	O231	102.10(14)	S3	O341	S4	123.96(17)
O31	S3	O32	122.9(2)				

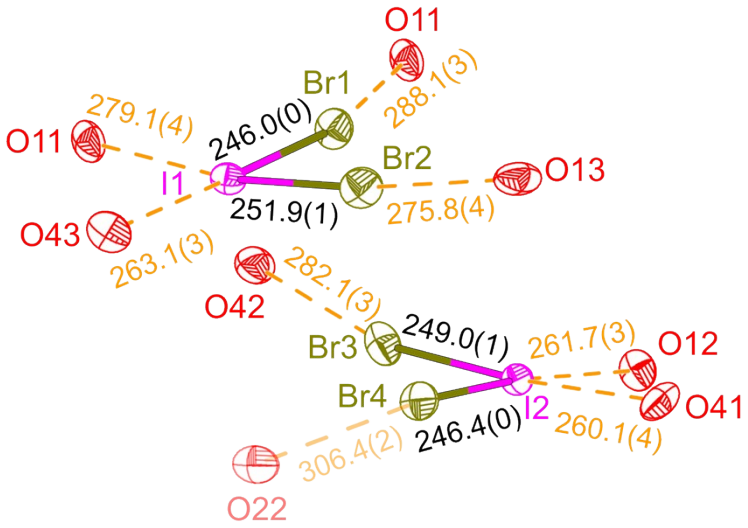

Figure S4: Coordination of the $[IBr_2]^+$ cations in the compound $[IBr_2]_2[S_4O_{13}]$. I–Br bond lengths are shown in black, Hal–O distances in orange. All distances are given in pm. Atoms with distances above 300 pm are set at 50% visibility. Thermal ellipsoids shown at 70% probability.

Table S6: Torsion Angles for $[IBr_2]_2[S_4O_{13}]$.

A	B	C	D	Angle/˚	A	B	C	D	Angle/˚
O11	S1	O121	S2	79.8(2)	O32	S3	O231	S2	–177.0(2)
O12	S1	O121	S2	–39.1(3)	O32	S3	O341	S4	38.5(3)
O13	S1	O121	S2	–160.4(2)	O41	S4	O341	S3	–77.9(2)
O21	S2	O121	S1	–169.6(2)	O42	S4	O341	S3	162.4(2)
O21	S2	O231	S3	35.5(3)	O43	S4	O341	S3	41.9(2)
O22	S2	O121	S1	54.9(3)	O121	S2	O231	S3	–76.9(2)
O22	S2	O231	S3	166.8(2)	O231	S2	O121	S1	–54.9(2)
O31	S3	O231	S2	51.5(3)	O231	S3	O341	S4	–70.7(2)
O31	S3	O341	S4	175.2(2)	O341	S3	O231	S2	–60.9(2)

$[I_3]_4[S_4O_{13}]_2(SO_3)$

Table S7: Crystallographic data of $[I_3]_4[S_4O_{13}]_2(SO_3)$.

Empirical formula	$I_{12}O_{29}S_9$
Formula weight	2275.34 g/mol
Temperature	100.00 K
Crystal system	monoclinic
Space group	*Cc* (No. 9)
Unit cell dimensions	*a* = 1535.60(8) pm *b* = 1391.60(8) pm *c* = 2087.85(13) pm *β* = 103.504(2)°
Volume	4338.3(4) Å^3
Z	4
ρ_{calc}	3.484 g/cm^3
μ	9.081 mm^{-1}
F(000)	4048
Crystal size	0.25 × 0.22 × 0.12 mm^3
Radiation	MoK_α (λ = 0.71073 nm)
2Θ range for data collection	4 to 63.088
Index ranges	-22 ≤ h ≤ 19, -19 ≤ k ≤ 20, -30 ≤ l ≤ 29
Reflections collected	67302
Independent reflections	12738 [R_{int} = 0.0468, R_σ = 0.0408]
Completeness to Θ = 50.5°	100%
Absorption correction	multiscan
Min. and max. transmission	0.327 / 0.746
Data/restraints/parameters	12738/2/451
Goodness-of-fit on F^2	1.194
Final R indexes [I>=2σ (I)]	R_1 = 0.0387, wR_2 = 0.0832
Final R indexes [all data]	R_1 = 0.0409, wR_2 = 0.0838
Largest diff. peak/hole	2.27/–1.65 e · Å^{-3}
Flack parameter	0.039(8)
CCDC-No.	2405913

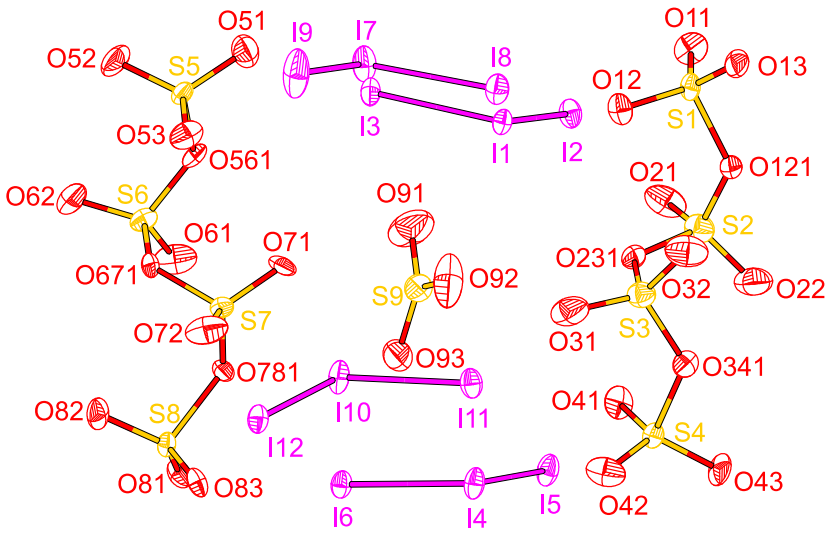

Figure S5: ORTEP of the asymmetric unit of $[I_3]_4[S_4O_{13}]_2(SO_3)$. Thermal ellipsoids shown with 70% probability.

Table S8: Fractional Atomic Coordinates (×10⁴) and Equivalent Isotropic Displacement Parameters (Å²×10³) for $[I_3]_4[S_4O_{13}]_2(SO_3)$. U_{eq} is defined as 1/3 of the trace of the orthogonalised U_{IJ} tensor.

Atom	*x*	*y*	*z*	U(eq)	Atom	*x*	*y*	*z*	U(eq)
I1	4420.8(5)	2673.2(5)	3263.5(4)	11.27(12)	O43	1653(6)	4325(7)	6757(5)	19.6(18)
I2	3116.1(5)	3907.4(5)	3357.3(4)	14.45(14)	O121	703(6)	5148(6)	4023(4)	15.2(16)
I3	5682.1(5)	3983.2(5)	3190.6(4)	14.23(14)	O231	2081(6)	5338(6)	4912(4)	16.5(17)
I4	5765.7(5)	1624.4(5)	6521.1(4)	14.61(15)	O341	2010(6)	4026(6)	5722(4)	15.3(16)
I5	4398.5(5)	2804.0(5)	6560.8(4)	16.68(15)	S5	7704(2)	5396(2)	3434.7(14)	13.4(5)
I6	7109.3(5)	2900.1(5)	6736.5(4)	12.73(13)	S6	8167(2)	6233(2)	4755.7(14)	15.2(5)
I7	4364.0(5)	8193.7(5)	3545.9(5)	19.15(16)	S7	7879.9(19)	4414.4(19)	5306.1(13)	12.6(5)
I8	3082.8(5)	6875.8(5)	3573.1(4)	16.61(15)	S8	8710.3(18)	4847.3(18)	6668.7(14)	10.7(5)
I9	5670.3(6)	6963.0(6)	3464.5(6)	32.5(2)	O51	6804(7)	5395(7)	3031(5)	25(2)
I10	5390.7(5)	7767.7(5)	6441.3(4)	15.68(15)	O52	8324(8)	6023(8)	3230(5)	28(2)
I11	4079.1(5)	6456.3(5)	6288.7(4)	14.74(14)	O53	8024(7)	4464(6)	3692(5)	20.8(19)
I12	6879.7(5)	6668.7(5)	6684.8(4)	13.81(14)	O61	7692(8)	6644(7)	5185(5)	26(2)
S1	1025.3(19)	5364.5(19)	3304.4(15)	12.3(5)	O62	8942(7)	6652(8)	4630(5)	28(2)
S2	1053(2)	5691(2)	4684.8(16)	18.6(6)	O71	6997(6)	4453(7)	4910(4)	21.1(19)
S3	2400(2)	4239(2)	5107.4(15)	16.9(5)	O72	8392(8)	3568(7)	5399(5)	28(2)
S4	2389.0(19)	4563.8(18)	6479.5(14)	11.7(5)	O81	8371(6)	5546(6)	7046(4)	15.7(16)
O11	656(7)	6279(6)	3078(5)	21.3(19)	O82	9474(6)	5110(6)	6427(5)	17.8(17)
O12	1989(6)	5352(6)	3521(5)	16.1(17)	O83	8691(5)	3863(6)	6879(4)	13.4(15)
O13	642(6)	4526(7)	2956(4)	21.4(19)	O561	7466(6)	5985(6)	4109(4)	14.9(16)
O21	1132(7)	6686(7)	4579(5)	27(2)	O671	8504(5)	5164(6)	5028(4)	12.7(15)
O22	562(7)	5306(8)	5125(5)	28(2)	O781	7823(5)	4883(6)	5971(4)	12.9(15)
O31	3343(7)	4310(8)	5282(5)	29(2)	S9	5233(2)	4504(2)	5110.3(16)	19.9(6)
O32	1930(8)	3611(7)	4596(5)	30(2)	O91	4980(9)	5264(10)	4659(7)	48(3)
O41	2465(7)	5561(6)	6320(5)	19.0(18)	O92	5129(8)	3552(9)	4899(7)	41(3)
O42	3234(7)	4075(7)	6757(5)	23(2)	O93	5560(7)	4713(8)	5779(5)	29(2)

Table S9: Anisotropic Displacement Parameters (Å²×10³) for $[I_3]_4[S_4O_{13}]_2(SO_3)$. The anisotropic displacement factor exponent takes the form: $-2\pi^2[h^2a^{*2}U_{11}+2hka^*b^*U_{12}+\ldots]$.

Atom	U_{11}	U_{22}	U_{33}	U_{23}	U_{13}	U_{12}
I1	9.4(3)	9.7(3)	15.6(3)	0.2(2)	4.7(2)	–0.1(2)
I2	10.3(3)	14.9(3)	18.6(3)	–3.1(3)	4.3(3)	1.6(2)
I3	10.7(3)	15.0(3)	17.7(3)	–3.0(3)	4.8(3)	–3.3(3)
I4	11.3(3)	9.5(3)	24.3(4)	–0.2(3)	6.7(3)	–0.7(2)
I5	10.8(3)	14.3(3)	26.4(4)	4.4(3)	7.2(3)	2.1(3)
I6	11.1(3)	8.8(3)	18.6(3)	0.9(2)	4.3(3)	–0.2(2)
I7	13.3(3)	11.2(3)	32.4(4)	1.6(3)	4.2(3)	0.0(3)
I8	13.2(3)	13.5(3)	23.3(4)	1.9(3)	4.7(3)	0.0(3)
I9	13.8(4)	19.0(4)	65.3(7)	13.1(4)	10.3(4)	5.2(3)
I10	11.1(3)	10.1(3)	27.2(4)	–0.2(3)	7.0(3)	–0.3(2)
I11	11.5(3)	11.5(3)	20.8(4)	–1.3(3)	3.1(3)	–0.2(2)
I12	10.5(3)	13.4(3)	18.5(3)	–2.3(3)	5.4(3)	–0.8(2)
S1	7.6(12)	11.9(11)	18.0(13)	0.6(10)	4.6(10)	2.6(9)
S2	16.7(14)	19.3(13)	19.3(14)	0.7(11)	3.3(11)	5.8(11)
S3	17.6(14)	17.5(13)	15.7(12)	1.1(10)	4.3(11)	2.6(10)
S4	10.9(12)	9.7(10)	15.3(12)	0.0(9)	4.8(10)	0.8(9)
O11	23(5)	16(4)	26(5)	3(3)	9(4)	8(4)
O12	12(4)	11(4)	24(4)	1(3)	2(3)	3(3)
O13	17(4)	34(5)	15(4)	–7(4)	8(3)	–8(4)
O21	34(6)	14(4)	26(5)	3(4)	–5(4)	9(4)
O22	29(6)	39(6)	18(5)	4(4)	7(4)	8(4)
O31	25(5)	38(6)	26(5)	15(4)	10(4)	15(4)
O32	42(6)	24(5)	22(5)	–3(4)	5(4)	4(4)
O41	25(5)	7(3)	25(5)	–4(3)	4(4)	–7(3)
O42	27(5)	22(4)	20(4)	0(4)	3(4)	14(4)
O43	13(4)	26(4)	23(4)	–4(4)	12(3)	–1(3)
O121	13(4)	20(4)	12(4)	–1(3)	3(3)	–4(3)
O231	15(4)	17(4)	16(4)	6(3)	3(3)	–2(3)
O341	20(4)	11(3)	15(4)	–5(3)	6(3)	–5(3)
S5	14.7(14)	14.2(12)	12.4(12)	1.6(9)	5.3(10)	–4.4(10)
S6	19.1(14)	13.5(12)	14.1(12)	3.2(10)	5.9(11)	–0.2(10)
S7	13.6(12)	12.8(11)	11.0(12)	2.7(9)	2.1(10)	–0.7(9)
S8	8.1(11)	9.7(10)	14.8(13)	0.8(9)	3.6(9)	–0.1(9)
O51	18(5)	23(5)	29(5)	8(4)	–1(4)	–3(4)
O52	37(6)	31(5)	21(5)	–4(4)	13(4)	–23(4)
O53	30(5)	15(4)	19(4)	–1(3)	10(4)	–2(4)
O61	40(6)	17(4)	23(5)	3(4)	10(4)	11(4)
O62	29(6)	34(5)	24(5)	5(4)	11(4)	–11(4)
O71	21(5)	27(5)	10(4)	4(3)	–6(3)	–9(4)
O72	40(6)	26(5)	21(5)	6(4)	11(4)	9(4)
O81	10(4)	19(4)	17(4)	–4(3)	1(3)	3(3)
O82	15(4)	12(4)	26(5)	3(3)	3(3)	–5(3)
O83	8(4)	13(4)	18(4)	–4(3)	0(3)	1(3)
O561	16(4)	18(4)	14(4)	2(3)	10(3)	–1(3)
O671	6(3)	17(4)	15(4)	1(3)	2(3)	0(3)
O781	12(4)	14(4)	11(4)	1(3)	–1(3)	–3(3)
S9	18.1(15)	24.8(14)	17.5(14)	–0.4(11)	5.5(12)	–0.1(11)
O91	39(7)	63(9)	45(7)	33(7)	16(6)	19(6)
O92	28(6)	40(6)	61(8)	–26(6)	23(6)	–13(5)
O93	20(5)	48(6)	20(5)	–5(4)	5(4)	–5(4)

Table S10: Bond Lengths for $[I_3]_4[S_4O_{13}]_2(SO_3)$.

Atom	Atom	Length/pm	Atom	Atom	Length/pm
I1	I2	268.07(10)	S4	O43	142.4(9)
I1	I3	268.98(10)	S4	O341	172.3(9)
I4	I5	268.15(10)	S5	O51	144.0(10)
I4	I6	267.90(10)	S5	O52	142.9(10)
I7	I9	267.30(12)	S5	O53	144.6(10)
I8	I7	269.99(11)	S5	O561	174.0(9)
I10	I11	268.12(10)	S6	O61	140.3(10)
I12	I10	269.87(10)	S6	O62	140.5(10)
S1	O11	142.8(9)	S6	O561	155.6(9)
S1	O12	144.3(9)	S6	O671	163.3(9)
S1	O13	142.7(10)	S7	O71	141.5(9)
S1	O121	171.2(9)	S7	O72	140.4(10)
S2	O21	141.2(10)	S7	O671	161.3(9)
S2	O22	142.1(11)	S7	O781	155.5(9)
S2	O121	155.7(9)	S8	O81	142.4(9)
S2	O231	161.6(10)	S8	O82	142.9(9)
S3	O31	141.2(11)	S8	O83	144.0(8)
S3	O32	143.8(11)	S8	O781	174.7(8)
S3	O231	162.8(9)	S9	O91	140.8(12)
S3	O341	156.7(9)	S9	O92	139.3(12)
S4	O41	143.9(8)	S9	O93	139.9(10)
S4	O42	146.0(10)			

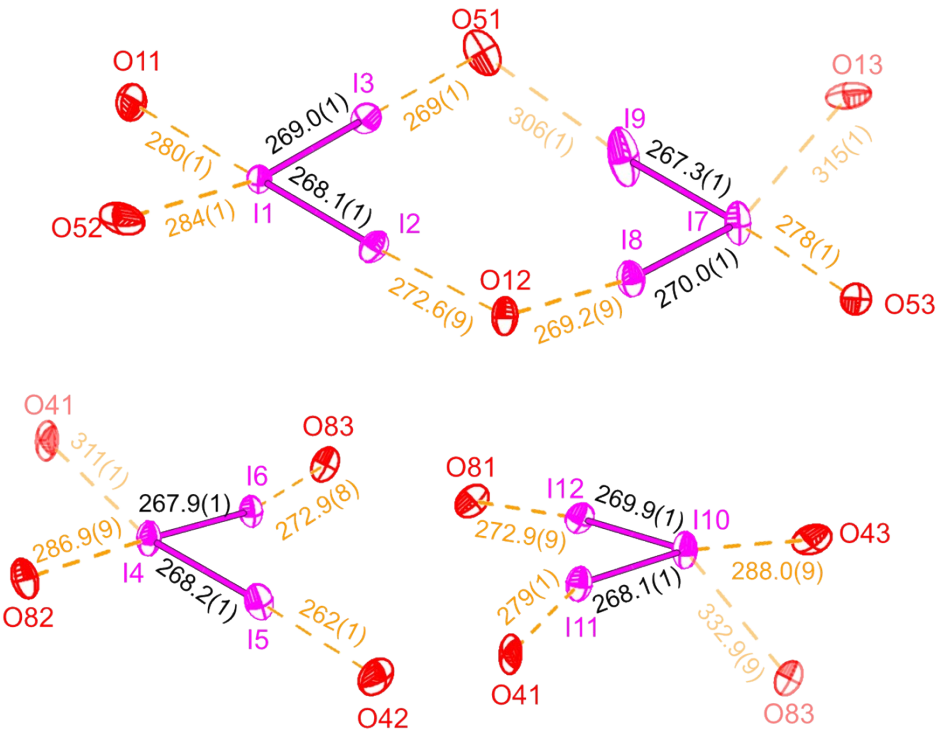

Figure S6: Coordination of the $[I_3]^+$ cations in the compound $[I_3]_4[S_4O_{13}]_2(SO_3)$. I–I bond lengths are shown in black, I–O distances in orange. All distances are given in pm. Atoms with distances above 300 pm are set at 50% visibility. Thermal ellipsoids shown at 70% probability.

Table S11: Bond Angles for $[I_3]_4[S_4O_{13}]_2(SO_3)$.

Atom	Atom	Atom	Angle/˚	Atom	Atom	Atom	Angle/˚
I2	I1	I3	97.48(3)	O51	S5	O53	114.4(6)
I6	I4	I5	99.61(3)	O51	S5	O561	96.9(6)
I9	I7	I8	97.32(3)	O52	S5	O51	116.1(6)
I11	I10	I12	102.51(3)	O52	S5	O53	117.8(7)
O11	S1	O12	114.4(6)	O52	S5	O561	103.6(5)
O11	S1	O121	105.9(5)	O53	S5	O561	103.9(5)
O12	S1	O121	102.1(5)	O61	S6	O62	122.6(7)
O13	S1	O11	118.4(6)	O61	S6	O561	106.7(6)
O13	S1	O12	114.9(6)	O61	S6	O671	108.6(5)
O13	S1	O121	97.7(5)	O62	S6	O561	112.0(5)
O21	S2	O22	123.3(7)	O62	S6	O671	103.3(6)
O21	S2	O121	111.2(5)	O561	S6	O671	101.5(4)
O21	S2	O231	103.3(6)	O71	S7	O671	109.5(5)
O22	S2	O121	105.4(6)	O71	S7	O781	105.1(5)
O22	S2	O231	108.9(5)	O72	S7	O71	122.8(7)
O121	S2	O231	102.9(5)	O72	S7	O671	103.4(6)
O31	S3	O32	122.8(7)	O72	S7	O781	112.0(5)
O31	S3	O231	103.2(6)	O781	S7	O671	102.2(4)
O31	S3	O341	111.6(5)	O81	S8	O82	117.2(5)
O32	S3	O231	108.4(6)	O81	S8	O83	116.4(5)
O32	S3	O341	105.8(6)	O81	S8	O781	97.3(5)
O341	S3	O231	103.4(5)	O82	S8	O83	115.3(5)
O41	S4	O42	115.4(6)	O82	S8	O781	104.1(5)
O41	S4	O341	103.6(5)	O83	S8	O781	102.3(4)
O42	S4	O341	103.9(5)	S6	O561	S5	125.0(5)
O43	S4	O41	115.8(6)	S7	O671	S6	123.2(5)
O43	S4	O42	116.5(6)	S7	O781	S8	122.5(5)
O43	S4	O341	98.1(5)	O92	S9	O91	120.6(9)
S2	O121	S1	125.6(5)	O92	S9	O93	120.1(8)
S2	O231	S3	125.1(6)	O93	S9	O91	119.3(9)
S3	O341	S4	123.9(5)				

Table S12: Torsion Angles for $[I_3]_4[S_4O_{13}]_2(SO_3)$.

A	B	C	D	Angle/˚	A	B	C	D	Angle/˚
O11	S1	O121	S2	–69.8(8)	O51	S5	O561	S6	179.8(7)
O12	S1	O121	S2	50.2(8)	O52	S5	O561	S6	–61.1(8)
O13	S1	O121	S2	167.7(7)	O53	S5	O561	S6	62.5(7)
O21	S2	O121	S1	40.8(9)	O61	S6	O561	S5	–176.1(6)
O21	S2	O231	S3	179.5(7)	O61	S6	O671	S7	42.8(8)
O22	S2	O121	S1	176.7(7)	O62	S6	O561	S5	47.1(8)
O22	S2	O231	S3	46.9(9)	O62	S6	O671	S7	174.5(7)
O31	S3	O231	S2	–178.7(7)	O71	S7	O671	S6	40.1(8)
O31	S3	O341	S4	41.4(9)	O71	S7	O781	S8	170.3(6)
O32	S3	O231	S2	49.8(9)	O72	S7	O671	S6	172.5(7)
O32	S3	O341	S4	177.2(7)	O72	S7	O781	S8	34.7(8)
O41	S4	O341	S3	45.0(8)	O81	S8	O781	S7	167.2(6)
O42	S4	O341	S3	–75.9(8)	O82	S8	O781	S7	46.7(7)
O43	S4	O341	S3	164.1(7)	O83	S8	O781	S7	–73.6(7)
O121	S2	O231	S3	–64.7(7)	O561	S6	O671	S7	–69.4(7)
O231	S2	O121	S1	–69.2(7)	O671	S6	O561	S5	–62.5(7)
O231	S3	O341	S4	–68.9(7)	O671	S7	O781	S8	–75.4(6)
O341	S3	O231	S2	–62.2(8)	O781	S7	O671	S6	–71.0(7)

$[ICl_2][HS_2O_7]$

Table S13: Crystallographic data of $[ICl_2][HS_2O_7]$.

Empirical formula	$Cl_2HIO_7S_2$
Formula weight	374.93 g/mol
Temperature	104.00 K
Crystal system	triclinic
Space group	$P\bar{1}$ (No. 2)
Unit cell dimensions	a = 535.43(3) pm b = 849.43(5) pm c = 981.62(7) pm α = 82.489(2)° β = 78.136(2)° γ = 85.217(2)°
Volume	432.43(5) Å^3
Z	2
ρ_{calc}	2.879 g/cm^3
μ	4.800 mm^{-1}
F(000)	352
Crystal size	0.16 × 0.03 × 0.01 mm^3
Radiation	MoK_α (λ = 0.71073 nm)
2Θ range for data collection	4.27 to 80.588
Index ranges	-9 ≤ h ≤ 9, -15 ≤ k ≤ 15, -17 ≤ l ≤ 17
Reflections collected	56924
Independent reflections	5439 [R_{int} = 0.0391, R_σ = 0.0189]
Completeness to Θ = 50.5°	100%
Absorption correction	multiscan
Min. and max. transmission	0.586 / 0.748
Data/restraints/parameters	5439/1/113
Goodness-of-fit on F^2	1.096
Final R indexes [I>=2σ (I)]	R_1 = 0.0260, wR_2 = 0.0588
Final R indexes [all data]	R_1 = 0.0285, wR_2 = 0.0600
Largest diff. peak/hole	1.91/–1.37 e · Å^{-3}
CCDC-No.	2405909

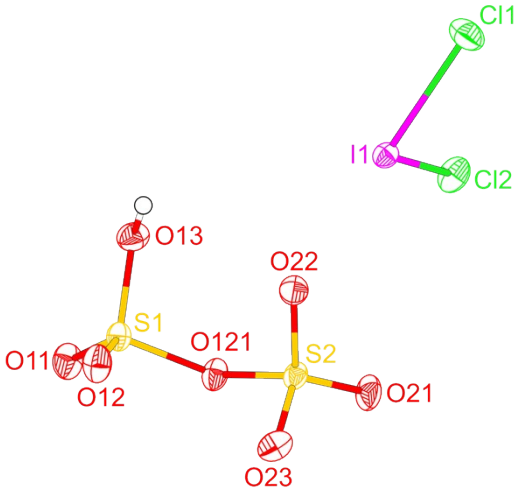

Figure S7: ORTEP of the asymmetric unit of $[ICl_2][HS_2O_7]$. Thermal ellipsoids shown with 70% probability.

Table S14: Fractional Atomic Coordinates (×10⁴) and Equivalent Isotropic Displacement Parameters (Å²×10³) for $[ICl_2][HS_2O_7]$. U_{eq} is defined as 1/3 of the trace of the orthogonalised U_{ij} tensor.

Atom	*x*	*y*	*z*	U(eq)
I1	5695.5(2)	1583.5(2)	2559.1(2)	10.04(3)
Cl1	7854.5(9)	1566.1(6)	301.0(5)	18.73(7)
Cl2	2433.1(8)	3282.7(5)	1959.4(5)	16.28(7)
S1	2996.5(7)	3518.8(5)	7641.5(4)	10.64(6)
S2	708.8(7)	1717.0(5)	6009.5(4)	11.00(6)
O11	1980(3)	4726.6(17)	8500.8(15)	16.0(2)
O12	3978(3)	2028.9(16)	8199.4(15)	16.0(2)
O13	4929(3)	4268.8(17)	6383.0(15)	15.0(2)
O21	-1421(2)	2205.7(19)	5336.5(15)	16.8(2)
O22	3203(2)	1700.4(18)	5102.0(14)	15.6(2)
O23	348(3)	314.6(16)	7021.6(16)	15.8(2)
O121	643(2)	3213.8(16)	6930.5(14)	12.88(19)

Table S15: Anisotropic Displacement Parameters (Å²×10³) for $[ICl_2][HS_2O_7]$. The anisotropic displacement factor exponent takes the form: $-2\pi^2[h^2a^{*2}U_{11}+2hka^*b^*U_{12}+\ldots]$.

Atom	U_{11}	U_{22}	U_{33}	U_{23}	U_{13}	U_{12}
I1	8.57(4)	9.99(4)	11.53(4)	−2.22(3)	−1.53(3)	0.04(3)
Cl1	18.54(17)	23.91(19)	12.00(15)	−1.62(13)	−0.05(12)	0.71(14)
Cl2	12.53(14)	14.55(15)	22.85(18)	−2.39(13)	−6.84(13)	1.70(11)
S1	11.14(13)	10.00(14)	11.52(14)	−2.55(11)	−3.58(11)	0.60(11)
S2	7.35(12)	14.34(15)	12.10(14)	−4.63(11)	−2.09(10)	0.13(11)
O11	16.7(5)	15.2(5)	17.5(5)	−7.8(4)	−3.7(4)	1.8(4)
O12	19.8(5)	11.8(5)	18.4(5)	−1.2(4)	−9.8(4)	1.5(4)
O13	12.1(5)	15.9(5)	16.3(5)	−2.7(4)	−0.7(4)	−1.3(4)
O21	10.1(4)	25.9(6)	16.5(5)	−6.8(5)	−6.0(4)	1.7(4)
O22	8.7(4)	24.6(6)	13.8(5)	−8.5(4)	0.7(4)	0.0(4)
O23	12.4(5)	13.6(5)	21.0(6)	−1.9(4)	−2.4(4)	−1.1(4)
O121	10.2(4)	14.4(5)	15.3(5)	−5.6(4)	−4.2(4)	2.0(4)

Table S16: Bond Lengths for $[ICl_2][HS_2O_7]$.

Atom	Atom	Length/pm	Atom	Atom	Length/pm
I1	Cl1	228.07(5)	S1	O121	161.43(13)
I1	Cl2	229.38(4)	S2	O21	143.80(14)
S1	O11	141.59(14)	S2	O22	144.51(13)
S1	O12	141.57(14)	S2	O23	144.68(15)
S1	O13	154.30(14)	S2	O121	164.77(13)

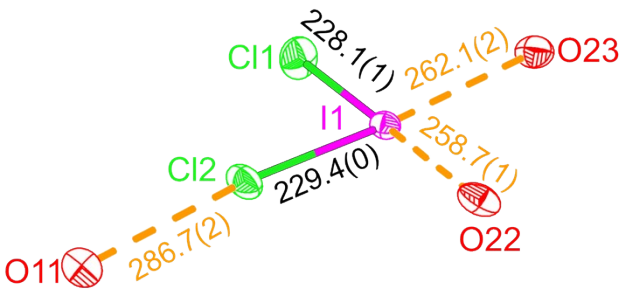

Figure S8: Coordination of the $[ICl_2]^+$ cations in the compound $[ICl_2][HS_2O_7]$. I–Cl bond lengths are shown in black, Hal–O distances in orange. All distances are given in pm. Thermal ellipsoids shown at 70% probability.

Table S17: Bond Angles for $[ICl_2][HS_2O_7]$.

Atom	Atom	Atom	Angle/˚	Atom	Atom	Atom	Angle/˚
Cl1	I1	Cl2	93.896(18)	O21	S2	O22	116.03(9)
O11	S1	O13	107.86(8)	O21	S2	O23	114.83(9)
O11	S1	O121	103.33(8)	O21	S2	O121	100.19(8)
O12	S1	O11	121.81(9)	O22	S2	O23	112.90(9)
O12	S1	O13	111.12(9)	O22	S2	O121	105.20(8)
O12	S1	O121	108.25(8)	O23	S2	O121	105.70(8)
O13	S1	O121	102.54(7)	S1	O121	S2	122.37(8)

Table S18: Torsion Angles for $[ICl_2][HS_2O_7]$.

A	B	C	D	Angle/˚	A	B	C	D	Angle/˚
O11	S1	O121	S2	–170.63(10)	O21	S2	O121	S1	–165.83(10)
O12	S1	O121	S2	–40.20(12)	O22	S2	O121	S1	–45.11(12)
O13	S1	O121	S2	77.32(11)	O23	S2	O121	S1	74.58(11)

$[ICl_2]_2[S_2O_7]$

Table S19: Crystallographic data of $[ICl_2]_2[S_2O_7]$.

Empirical formula	$Cl_4I_2O_7S_2$
Formula weight	571.72 g/mol
Temperature	100.00 K
Crystal system	triclinic
Space group	$P\bar{1}$ (No. 2)
Unit cell dimensions	a = 792.12(5) pm b = 952.48(6) pm c = 966.28(2) pm α = 103.951(2)° β = 113.986(2)° γ = 100.298(2)°
Volume	614.13(7) Å^3
Z	2
ρ_{calc}	3.092 g/cm^3
μ	6.339 mm^{-1}
F(000)	524
Radiation	MoK_α (λ = 0.71073 nm)
2Θ range for data collection	4.638 to 63.01
Index ranges	-11 ≤ h ≤ 11, -13 ≤ k ≤ 13, -14 ≤ l ≤ 14
Reflections collected	33754
Independent reflections	4028 [R_{int} = 0.0503, R_σ = 0.0329]
Completeness to Θ = 50.5°	100%
Absorption correction	multiscan
Min. and max. transmission	0.5661 / 0.7465
Data/restraints/parameters	4028/0/136
Goodness-of-fit on F^2	1.067
Final R indexes [I>=2σ (I)]	R_1 = 0.0350, wR_2 = 0.0649
Final R indexes [all data]	R_1 = 0.0404, wR_2 = 0.0683
Largest diff. peak/hole	1.90/–1.18 e · Å^{-3}
CCDC-No.	2405912

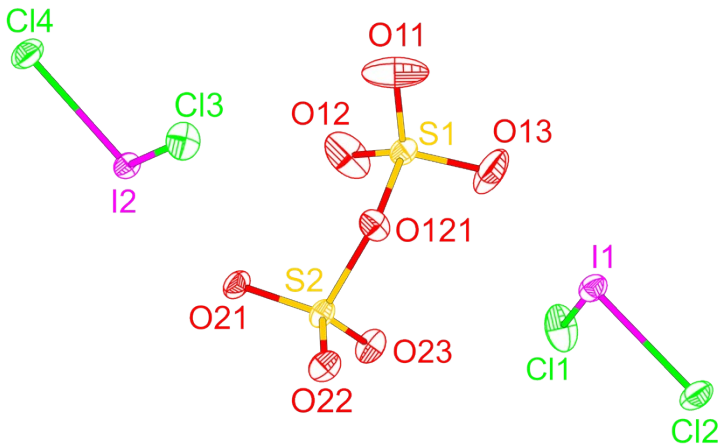

Figure S9: ORTEP of the asymmetric unit of $[ICl_2]_2[S_2O_7]$. Thermal ellipsoids shown with 50% probability.

Table S20: Fractional Atomic Coordinates (×10⁴) and Equivalent Isotropic Displacement Parameters (Å²×10³) for $[ICl_2]_2[S_2O_7]$. U_{eq} is defined as 1/3 of the trace of the orthogonalised U_{ij} tensor.

Atom	*x*	*y*	*z*	U(eq)
I1	42.2(4)	2028.2(3)	7591.0(3)	19.22(7)
Cl1	309.3(19)	4560.4(14)	8158.3(19)	37.2(3)
Cl2	228.7(16)	1997.8(13)	10027.6(12)	25.9(2)
S1	838.8(15)	2032.5(11)	4161.2(12)	17.90(18)
S2	4801.3(14)	3210.3(11)	6688.1(12)	16.41(18)
O11	94(7)	689(4)	2761(5)	52.0(12)
O12	1365(6)	3389(4)	3877(6)	46.8(11)
O13	-335(6)	2021(7)	4954(5)	59.7(15)
O21	5559(4)	3793(3)	5731(3)	20.4(6)
O22	5936(4)	2473(3)	7646(4)	20.7(6)
O23	4159(5)	4315(3)	7507(4)	22.7(6)
O121	2816(4)	1791(3)	5393(4)	21.3(6)
I2	5507.8(4)	3212.5(3)	3044.7(3)	16.20(7)
Cl3	4969.2(17)	752.3(11)	3053.9(14)	25.7(2)
Cl4	5479.1(17)	2454.8(12)	581.0(13)	25.9(2)

Table S21: Anisotropic Displacement Parameters (Å²×10³) for $[ICl_2]_2[S_2O_7]$. The anisotropic displacement factor exponent takes the form: $-2\pi^2[h^2a^{*2}U_{11}+2hka^*b^*U_{12}+\ldots]$.

Atom	U_{11}	U_{22}	U_{33}	U_{23}	U_{13}	U_{12}
I1	20.37(13)	25.14(13)	16.52(12)	9.8(1)	9.56(10)	11.31(10)
Cl1	38.6(6)	25.1(5)	62.1(9)	23.0(6)	30.8(6)	13.5(5)
Cl2	30.0(5)	34.8(6)	16.9(4)	12.1(4)	11.8(4)	13.1(4)
S1	22.3(5)	17.9(4)	16.5(4)	8.9(4)	9.7(4)	7.6(4)
S2	21.6(5)	17.0(4)	16.8(4)	10.0(3)	11.3(4)	8.7(4)
O11	66(3)	29.8(19)	29(2)	–1.9(16)	–4.5(19)	27(2)
O12	34(2)	37(2)	65(3)	41(2)	8.7(19)	8.0(16)
O13	36(2)	141(5)	35(2)	53(3)	25.6(19)	47(3)
O21	27.0(15)	19.2(13)	16.5(13)	8.0(11)	12.2(12)	3.0(11)
O22	27.0(15)	20.8(14)	20.5(14)	13.3(12)	11.4(12)	12.4(12)
O23	33.3(17)	19.6(14)	25.1(15)	10.6(12)	18.7(13)	14.5(12)
O121	20.6(14)	16.7(13)	26.4(15)	11.2(12)	9.0(12)	5.3(11)
I2	19.56(12)	15.11(11)	15.58(12)	6.26(9)	8.87(10)	6.39(9)
Cl3	33.0(5)	15.3(4)	33.3(6)	9.6(4)	18.6(5)	8.5(4)
Cl4	33.2(6)	26.3(5)	18.6(5)	4.1(4)	15.4(4)	7.8(4)

Table S22: Bond Lengths for $[ICl_2][S_2O_7]$.

Atom	Atom	Length/pm	Atom	Atom	Length/pm
I1	Cl1	229.08(12)	S2	O21	145.0(3)
I1	Cl2	230.60(10)	S2	O22	142.1(3)
I1	O13	244.0(4)	S2	O23	145.2(3)
S1	O11	143.6(4)	S2	O121	164.0(3)
S1	O12	141.1(3)	I2	Cl3	230.85(10)
S1	O13	142.5(4)	I2	Cl4	230.44(10)
S1	O121	163.3(3)			

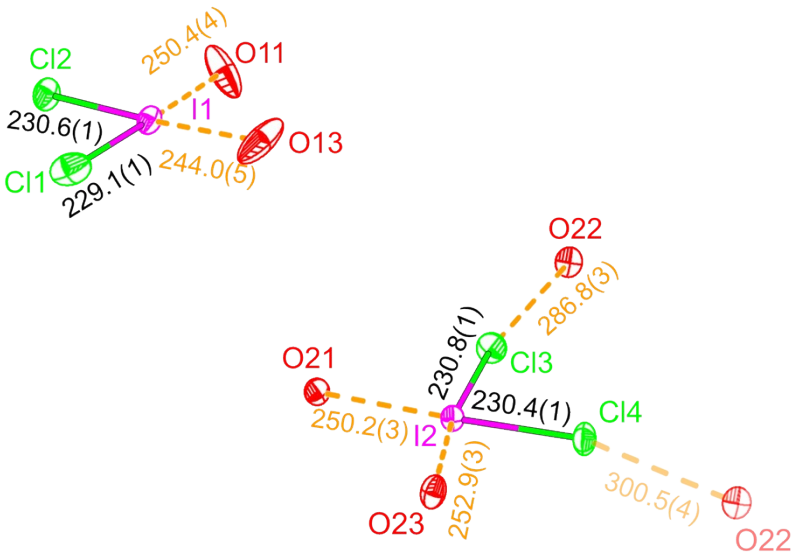

Figure S10: Coordination of the $[ICl_2]^+$ cations in the compound $[ICl_2]_2[S_2O_7]$. I–Cl bond lengths are shown in black, Hal–O distances in orange. All distances are given in pm. Atoms with distances above 300 pm are set at 50% visibility. Thermal ellipsoids shown at 70% probability.

Table S23: Bond Angles for $[ICl_2][S_2O_7]$.

Atom	Atom	Atom	Angle/°	Atom	Atom	Atom	Angle/°
Cl1	I1	Cl2	94.46(5)	O21	S2	O23	111.45(18)
Cl1	I1	O13	85.68(15)	O21	S2	O121	106.01(17)
Cl2	I1	O13	177.08(10)	O22	S2	O21	115.51(18)
O11	S1	O121	101.5(2)	O22	S2	O23	115.73(18)
O12	S1	O11	113.1(3)	O22	S2	O121	101.49(17)
O12	S1	O13	115.6(3)	O23	S2	O121	105.02(18)
O12	S1	O121	108.45(19)	S1	O13	I1	137.2(2)
O13	S1	O11	112.5(3)	S1	O121	S2	122.81(18)
O13	S1	O121	104.16(19)	Cl4	I2	Cl3	91.52(4)

Table S24: Torsion Angles for $[ICl_2][S_2O_7]$.

A	B	C	D	Angle/°	A	B	C	D	Angle/°
O11	S1	O13	I1	117.5(5)	O21	S2	O121	S1	–69.0(3)
O11	S1	O121	S2	145.7(3)	O22	S2	O121	S1	170.0(2)
O12	S1	O13	I1	–110.4(5)	O23	S2	O121	S1	49.1(3)
O12	S1	O121	S2	26.3(3)	O121	S1	O13	I1	8.4(6)
O13	S1	O121	S2	–97.4(3)					

$Li_2[S_4O_{13}]$

Table S25: Crystallographic data of $Li_2[S_4O_{13}]$.

Empirical formula	$Li_2O_{13}S_4$
Formula weight	350.12 g/mol
Temperature	100.00 K
Crystal system	monoclinic
Space group	$P2_1/n$ (No. 14)
Unit cell dimensions	a = 516.07(4) pm b = 2195.73(15) pm c = 880.70(6) pm α = 90° β = 94.233(3) γ = 90°
Volume	995.24(12) Å^3
Z	4
ρ_{calc}	2.337 g/cm^3
μ	1.027 mm^{-1}
F(000)	696
Radiation	MoK_α (λ = 0.71073 nm)
Crystal size	0.24 x 0.04 x 0.01 mm^3
2Θ range for data collection	4.996 to 56.608
Index ranges	-6 ≤ h ≤ 6, -29 ≤ k ≤ 29, -11 ≤ l ≤ 11
Reflections collected	15454
Independent reflections	2462 [R_{int} = 0.0691, R_σ = 0.0461]
Completeness to Θ = 50.5°	100%
Absorption correction	multiscan
Min. and max. transmission	0.6589 / 0.7457
Data/restraints/parameters	2462/0/172
Goodness-of-fit on F^2	1.068
Final R indexes [I>=2σ (I)]	R_1 = 0.0371, wR_2 = 0.0809
Final R indexes [all data]	R_1 = 0.0610, wR_2 = 0.0961
Largest diff. peak/hole	0.54/–0.59 e · Å^{-3}
CCDC-No.	2405910

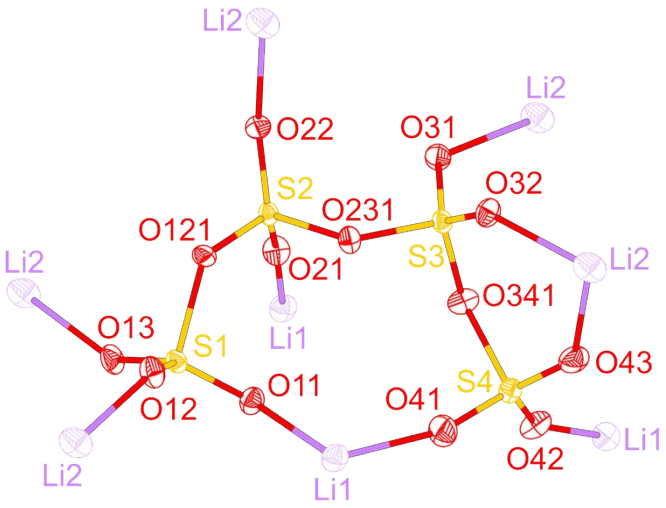

Figure S11: ORTEP of the asymmetric unit of $Li_2[S_4O_{13}]$. Thermal ellipsoids shown with 70% probability.

Table S26: Fractional Atomic Coordinates (×10⁴) and Equivalent Isotropic Displacement Parameters (Å²×10³) for $Li_2[S_4O_{13}]$. U_{eq} is defined as 1/3 of the trace of the orthogonalised U_{IJ} tensor.

Atom	*x*	*y*	*z*	U(eq)
S1	5859.2(14)	6165.9(4)	5505.0(9)	8.74(17)
S2	8581.3(14)	5597.6(4)	3081.4(8)	8.15(17)
S3	6627.9(14)	5873.9(4)	70.6(8)	8.68(17)
S4	3943.4(14)	7054.5(4)	-239.1(9)	9.99(17)
O11	5412(4)	6628.7(10)	4372(2)	12.0(5)
O121	6980(4)	5545.2(10)	4461(2)	10.3(4)
O13	7996(4)	6262.3(10)	6595(3)	13.1(5)
O12	3602(4)	5883.7(11)	6027(3)	13.1(5)
O231	6162(4)	5703.9(10)	1816(2)	10.3(5)
O21	10143(4)	6124.2(10)	3103(3)	12.5(5)
O22	9702(4)	5025.7(10)	2815(3)	11.6(5)
O341	6629(4)	6571.5(10)	99(3)	11.9(5)
O32	4418(4)	5631.3(10)	-751(3)	12.1(5)
O31	9172(4)	5687.3(10)	-222(3)	13.1(5)
O41	2795(5)	7039.2(11)	1178(3)	17.2(5)
O42	5356(4)	7589.6(10)	-541(3)	14.5(5)
O43	2490(4)	6785.1(11)	-1499(3)	15.8(5)
Li1	2191(10)	6880(3)	3240(6)	13.0(11)
Li2	1236(11)	5920(3)	7778(7)	16.4(12)

Table S27: Anisotropic Displacement Parameters (Å²×10³) for $Li_2[S_4O_{13}]$. The anisotropic displacement factor exponent takes the form: $-2\pi^2[h^2a^{*2}U_{11}+2hka^*b^*U_{12}+\ldots]$.

Atom	U_{11}	U_{22}	U_{33}	U_{23}	U_{13}	U_{12}
S1	7.4(3)	11.4(4)	7.4(4)	–1.0(3)	0.0(3)	0.5(3)
S2	7.0(3)	10.4(4)	7.0(4)	0.0(3)	–0.3(3)	0.0(3)
S3	7.7(3)	11.1(4)	7.2(4)	–0.2(3)	–0.1(3)	0.6(3)
S4	9.4(4)	10.6(4)	10.0(4)	1.3(3)	0.8(3)	0.2(3)
O11	10.5(11)	13.8(12)	11.6(11)	1.5(9)	–0.3(9)	1.0(9)
O121	11.9(11)	10.3(11)	9.2(11)	0.1(9)	3.9(8)	2.0(8)
O13	12.4(11)	17.3(12)	9.1(11)	–2.8(9)	–2.7(9)	–0.6(9)
O12	10.3(11)	18.7(12)	10.3(11)	0.0(9)	1.2(8)	–2.0(9)
O231	6.9(10)	15.0(12)	9.1(11)	0.5(9)	0.5(8)	–0.3(8)
O21	10.5(11)	13.8(12)	13.1(11)	–0.2(9)	0.0(9)	–2.8(9)
O22	10.8(11)	12.3(11)	11.6(11)	–0.4(9)	0.6(8)	2.7(9)
O341	7.8(10)	10.0(11)	18.0(12)	0.2(9)	0.5(9)	–1.5(8)
O32	10.4(11)	12.9(12)	12.5(11)	1.3(9)	–2.0(9)	–0.7(9)
O31	10.7(11)	17.4(12)	11.4(11)	0.9(9)	3.0(9)	4.0(9)
O41	16.1(12)	22.0(13)	14.1(12)	2.8(10)	5.3(9)	3.2(10)
O42	12.2(11)	12.1(12)	19.4(12)	3.6(9)	1.6(9)	1.3(9)
O43	13.8(11)	14.7(12)	17.8(12)	–2.0(9)	–4.5(9)	3.5(9)
Li1	10(2)	15(3)	14(3)	1(2)	0(2)	1(2)
Li2	10(3)	21(3)	18(3)	–3(2)	3(2)	0(2)

Table S28: Bond Lengths for $Li_2[S_4O_{13}]$.

Atom	Atom	Length/pm	Atom	Atom	Length/pm
S1	O11	143.1(2)	S4	O41	142.1(2)
S1	O121	176.5(2)	S4	O42	141.8(2)
S1	O13	142.4(2)	S4	O43	142.1(2)
S1	O12	142.5(2)	O11	Li1	195.4(6)
S2	O121	152.4(2)	O13	Li2[1]	204.6(6)
S2	O231	162.8(2)	O12	Li2	203.8(6)
S2	O21	140.9(2)	O21	Li1[1]	196.7(6)
S2	O22	141.0(2)	O22	Li2[2]	218.7(6)
S3	O231	161.7(2)	O32	Li2[3]	211.3(6)
S3	O341	153.2(2)	O31	Li2[4]	218.5(6)
S3	O32	140.9(2)	O41	Li1	189.8(6)
S3	O31	141.7(2)	O42	Li1[5]	188.5(6)
S4	O341	175.3(2)	O43	Li2[3]	209.0(6)

[1]1+X,+Y,+Z; [2]1-X,1-Y,1-Z; [3]+X,+Y,-1+Z; [4]1+X,+Y,-1+Z; [5]1/2+X,3/2-Y,-1/2+Z

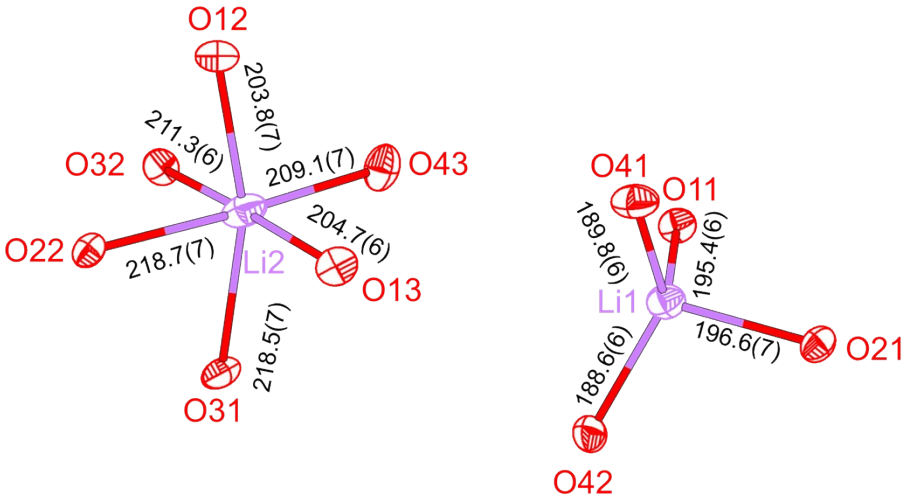

Figure S12: Coordination of the Li^+ cations in the compound $Li_2[S_4O_{13}]$ and Li–O distances in pm. Thermal ellipsoids shown at 70% probability.

Table S29: Bond Angles for $Li_2[S_4O_{13}]$.

Atom	Atom	Atom	Angle/˚	Atom	Atom	Atom	Angle/˚
O11	S1	O121	103.15(12)	S2	O21	Li1[1]	176.3(2)
O13	S1	O11	116.23(14)	S2	O22	Li2[2]	143.1(2)
O13	S1	O121	101.46(12)	S3	O341	S4	127.08(14)
O13	S1	O12	117.26(14)	S3	O32	Li2[3]	139.8(2)
O12	S1	O11	116.10(14)	S3	O31	Li2[4]	126.3(2)
O12	S1	O121	98.00(13)	S4	O41	Li1	162.5(2)
O121	S2	O231	97.09(12)	S4	O42	Li1[5]	154.8(2)
O21	S2	O121	113.23(13)	S4	O43	Li2[3]	138.6(2)
O21	S2	O231	107.51(13)	O11	Li1	O21[6]	103.0(3)
O21	S2	O22	119.48(14)	O41	Li1	O11	110.3(3)
O22	S2	O121	108.59(13)	O41	Li1	O21[6]	102.8(3)
O22	S2	O231	108.48(13)	O42[7]	Li1	O11	109.2(3)
O341	S3	O231	102.43(12)	O42[7]	Li1	O21[6]	105.4(3)
O32	S3	O231	103.24(13)	O42[7]	Li1	O41	123.8(3)
O32	S3	O341	112.67(13)	O13[6]	Li2	O22[2]	94.0(2)
O32	S3	O31	121.54(14)	O13[6]	Li2	O32[8]	172.4(3)
O31	S3	O231	108.13(13)	O13[6]	Li2	O31[9]	93.9(2)
O31	S3	O341	107.02(13)	O13[6]	Li2	O43[8]	92.6(3)
O41	S4	O341	102.25(13)	O12	Li2	O13[6]	98.2(3)
O41	S4	O43	116.45(15)	O12	Li2	O22[2]	85.2(2)
O42	S4	O341	97.02(12)	O12	Li2	O32[8]	88.3(2)
O42	S4	O41	115.97(15)	O12	Li2	O31[9]	162.8(3)
O42	S4	O43	116.57(15)	O12	Li2	O43[8]	94.4(3)
O43	S4	O341	104.21(13)	O32[8]	Li2	O22[2]	90.5(2)
S1	O11	Li1	130.1(2)	O32[8]	Li2	O31[9]	80.7(2)
S2	O121	S1	125.08(14)	O31[9]	Li2	O22[2]	81.8(2)
S1	O13	Li2[1]	148.4(2)	O43[8]	Li2	O22[2]	173.4(3)
S1	O12	Li2	140.9(2)	O43[8]	Li2	O32[8]	82.9(2)
S3	O231	S2	121.58(14)	O43[8]	Li2	O31[9]	97.2(3)

[1]1+X,+Y,+Z; [2]1-X,1-Y,1-Z; [3]+X,+Y,-1+Z; [4]1+X,+Y,-1+Z; [5]1/2+X,3/2-Y,-1/2+Z; [6]-1+X,+Y,+Z; [7]-1/2+X,3/2-Y,1/2+Z; [8]+X,+Y,1+Z;
[9]-1+X,+Y,1+Z

Table S30: Torsion Angles for $Li_2[S_4O_{13}]$.

A	B	C	D	Angle/°	A	B	C	D	Angle/°
S4	O41	Li1	O11	17.1(10)	O21	S2	O22	$Li2^4$	–165.2(3)
S4	O41	Li1	$O21^1$	–92.3(8)	O22	S2	O121	S1	164.05(15)
S4	O41	Li1	$O42^2$	149.0(6)	O22	S2	O231	S3	–74.91(19)
O11	S1	O121	S2	32.6(2)	O341	S3	O231	S2	–91.39(17)
O11	S1	O13	$Li2^3$	–133.4(4)	O341	S3	O32	$Li2^5$	10.2(4)
O11	S1	O12	Li2	–98.4(4)	O341	S3	O31	$Li2^6$	–59.2(3)
O121	S1	O11	Li1	98.1(3)	O341	S4	O41	Li1	6.3(8)
O121	S1	O13	$Li2^3$	–22.4(4)	O341	S4	O42	$Li1^7$	81.2(5)
O121	S1	O12	Li2	152.6(3)	O341	S4	O43	$Li2^5$	44.4(3)
O121	S2	O231	S3	172.73(16)	O32	S3	O231	S2	151.39(16)
O121	S2	O22	$Li2^4$	62.8(4)	O32	S3	O341	S4	20.3(2)
O13	S1	O11	Li1	–151.8(3)	O32	S3	O31	$Li2^6$	72.1(3)
O13	S1	O121	S2	–88.12(19)	O31	S3	O231	S2	21.4(2)
O13	S1	O12	Li2	45.3(4)	O31	S3	O341	S4	156.37(17)
O12	S1	O11	Li1	–7.7(3)	O31	S3	O32	$Li2^5$	–118.7(3)
O12	S1	O121	S2	151.85(17)	O41	S4	O341	S3	79.9(2)
O12	S1	O13	$Li2^3$	82.9(4)	O41	S4	O42	$Li1^7$	–171.5(5)
O231	S2	O121	S1	–83.69(17)	O41	S4	O43	$Li2^5$	–67.4(4)
O231	S2	O22	$Li2^4$	–41.6(4)	O42	S4	O341	S3	–161.56(19)
O231	S3	O341	S4	–90.01(18)	O42	S4	O41	Li1	–97.9(8)
O231	S3	O32	$Li2^5$	120.0(3)	O42	S4	O43	$Li2^5$	149.9(3)
O231	S3	O31	$Li2^6$	–168.9(2)	O43	S4	O341	S3	–41.8(2)
O21	S2	O121	S1	28.8(2)	O43	S4	O41	Li1	119.1(8)
O21	S2	O231	S3	55.60(19)	O43	S4	O42	$Li1^7$	–28.6(6)

C. Spectroscopic Investigations

Infrared Spectroscopy (FT-IR) Measurements

All measurements were performed at room temperature under Argon atmosphere in a glove box with a *Bruker Alpha II* device using the *OPUS* software.[14] Absorption bands are given in the corresponding wavenumber $\tilde{\nu}$ (cm^{-1}). The data was plotted using the software *OriginPro*.[15]

Raman Spectroscopy Measurements

All spectra were recorded with an *inVia Qotor confocal Raman microscope*, equipped with 10x, 50x and 100x magnification lenses, from Renishaw GmbH (Pliezhausen, GER). The spectra were measured on selected single crystals samples at room temperature using a green laser (λ= 532 nm, 100 mW) and varying exposure times. The data was processed with the *WiRE 5.1* software.[16] The data was plotted using the software *OriginPro*.[15]

$[IBr_2]_2[S_4O_{13}]$

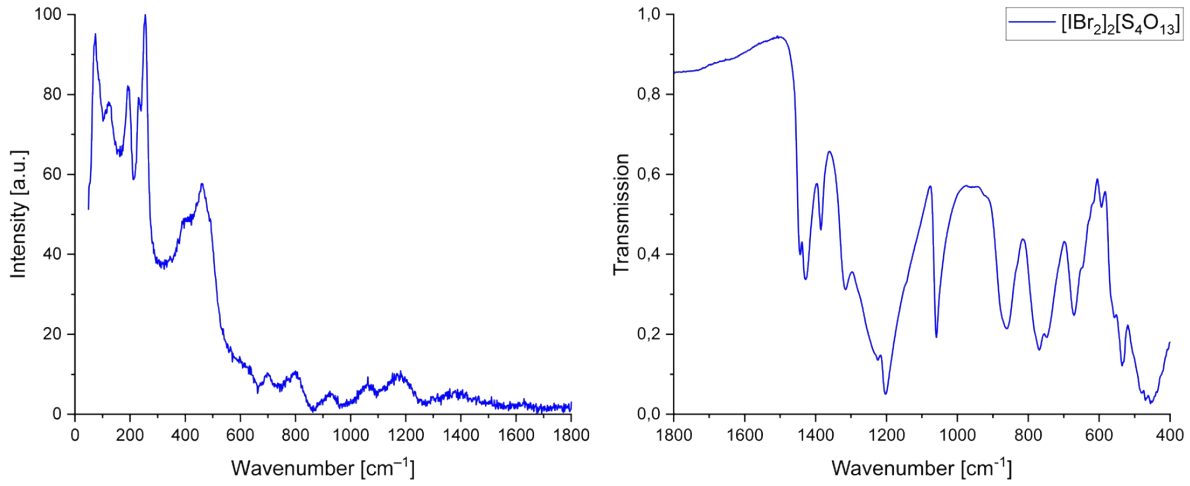

Figure S13: Raman (left) and IR (right) spectra of $[IBr_2]_2[S_4O_{13}]$.

Table S31*:* Raman frequencies (in cm^{-1}) of the $[IBr_2]^+$ cation in **1** compared to reference compounds and previously reported calculated values. DFT calculated values for the vibrational modes of the cations and before and after applying a shift factor for correction of the peak positions are coloured in magenta.

$[IBr_2][SO_3F]$[17]	$[IBr_2][Sb_2F_{11}]$[18]	$[IBr_2]_2[S_4O_{13}]$	$[IBr_2]^+$ [19]	$[S_4O_{13}]^{2-}$ [20]	Calculated *(shifted)*
256 (vs)	257	255 (s)	255 (ν_{sym})		203–271 (*253–321*) – $\nu_{as/sym}$
256 (vs)	232	230 (s, sh)			
198 (vw)	197	191 (s)			
127 (w, sh)	123	121 (s, sh)	100 (δ)		80 (*130*) – δ
		74 (s)			

vs = very strong, s = strong, m = medium, w = weak, vw = very weak, sh = shoulder, δ = bending, ν_{as} = asymmetric stretching, ν_{sym} = symmetric stretching

Table S32*:* Raman frequencies (in cm^{-1}) of $[IBr_2]_2[S_4O_{13}]$ compared to published quantum chemical calculated vibrational modes for the $[S_4O_{13}]^{2-}$ anion.

$[IBr_2]_2[S_4O_{13}]$	$[S_4O_{13}]^{2-}$ [20]	Vibrational mode
	1421	
	1409	
	1352	
	1245	
1181 (w, sh)		$\nu_{sym}(S{=}O_{inner})$
1062 (w)	1078	$\nu_{sym}(S{=}O_{term.})$
925 (w)	934	$\nu(S{-}O{-}S_{term.})$
805 (w)		
706 (w)	748	$\nu(S{-}O{-}S_{inner})$
464 (m)	398–623	$\delta(SO_3)$
418 (m, sh)		
255 (s)		
230 (s, sh)		$\nu_{as/sym}(IBr_2)$
191 (s)		
121 (s, sh)		$\delta(IBr_2)$
74 (s)		

s = strong, m = medium, w = weak, sh = shoulder, δ = bending, ν_{as} = asymmetric stretching, ν_{sym} = symmetric stretching

$[I_3]_4[S_4O_{13}]_2(SO_3)$

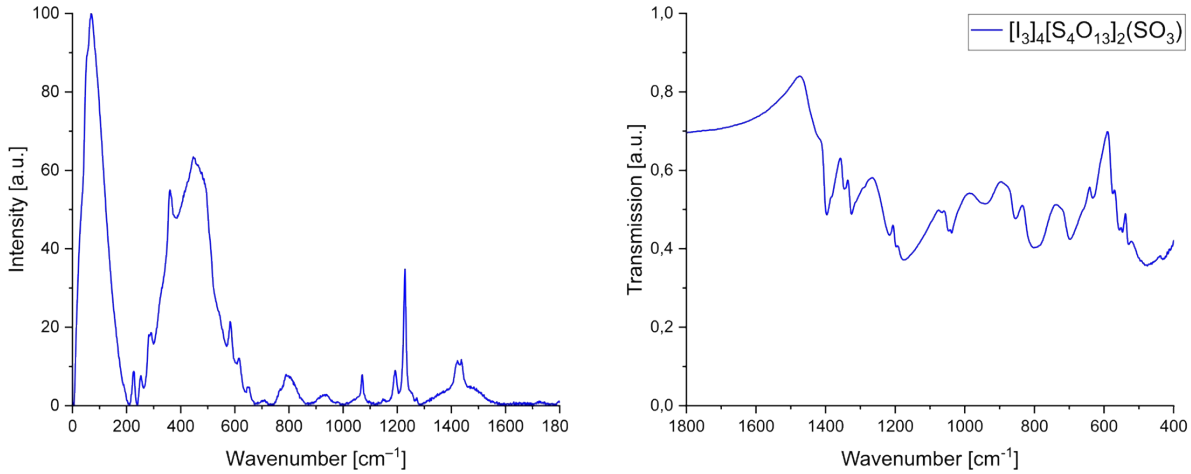

Figure S14: Raman (left) and IR (right) spectra of $[I_3]_4[S_4O_{13}]_2(SO_3)$.

Table S33: Raman frequencies (in cm^{-1}) of the $[I_3]^+$ cation in **2** compared to reference compounds and previously reported calculated values. DFT calculated values for the vibrational modes of the cations and before and after applying a shift factor for correction of the peak positions are coloured in magenta.

$[I_3][SO_3F]$[17]	$[I_3]_4[S_4O_{13}]_2(SO_3)$	$[I_3]^+$ [19]	Calculated *(shifted)*
364 (m)	360 (m, sh)		
	226 (w)	205 (MP: 202) (ν_{sym})	196–215 (236–*255*) – $\nu_{as/sym}$ (I_3)
	72 (s)	75 (MP: 95) (δ)	62–94 (*102–134*) – δ(I_3)

s = strong, m = medium, w = weak, sh = shoulder, , δ = bending, ν_{as} = asymmetric stretching, ν_{sym} = symmetric stretching, MP = Madelung Potential

Table S34: Raman frequencies (in cm^{-1}) of $[I_3]_4[S_4O_{13}]_2(SO_3)$ compared to published quantum chemical calculated vibrational modes for the $[S_4O_{13}]^{2-}$ anion.

$[I_3]_4[S_4O_{13}]_2(SO_3)$	$[S_4O_{13}]^{2-}$ [20]	Vibrational mode
1437 (w)	1421	$\nu_{as}(S{=}O_{inner})$
	1409	
	1352	
1229 (m)	1245	$\nu_{sym}(S{=}O_{inner})$
1192 (w, sh)		$\nu_{sym}(S{=}O_{term.})$
1071 (w)	1078	$\nu(S{-}O{-}S_{term.})$
935 (w)	934	
798 (w)	748	$\nu(S{-}O{-}S_{inner})$
584 (w, sh)		
448 (s)	398–623	δ(SO_3)
360 (m, sh)		$\nu_{as/sym}$ (I_3)
226 (w)		
72 (s)		δ(I_3)

s = strong, m = medium, w = weak, sh = shoulder, , δ = bending, ν_{as} = asymmetric stretching, ν_{sym} = symmetric stretching

D. Delta Values

General Procedure

The delta values (in the following written as δ) were calculated using the *Polynator* software package. Therein, δ is calculated as follows:

$$\delta = 100\left(\frac{\sum_i |a_i - v_i|^2}{\sum_i |a_i - c|^2}\right)^{1/2} \qquad (1.0)$$

where $\mathbf{a_i}$ is an atom vector, $\mathbf{v_i}$ is the vector the corresponding model vertex and **c** is the centroid of all atom vectors.[21]

The *.cif* files from the analyzed substances were taken from the ICSD/CCDC websites and used without further modification. Within the software, the central and ligand atoms were defined as sulfur and oxygen, respectively. The terminal SO_3 units could be identified in most cases by adjusting the distance connectivity criterium to a maximum value of 1.6 Å. For the analysis, the generated δ values for the geometric object 'triangle[regular] (–6m2, 1 °f' were taken. If 'tripod[3m] (2 °f)' would be chosen as the geometric object, the correction of the central atoms' distortion would lead to values not suitable for comparison.

As a reference for a trigonal planar, nearly uncoordinated SO_3 molecule, the free SO_3 unit within our compound $[I_3]_4[S_4O_{13}]_2(SO_3)$, i.e. S9, O91, O92 and O93, was used (see fig. S 15).

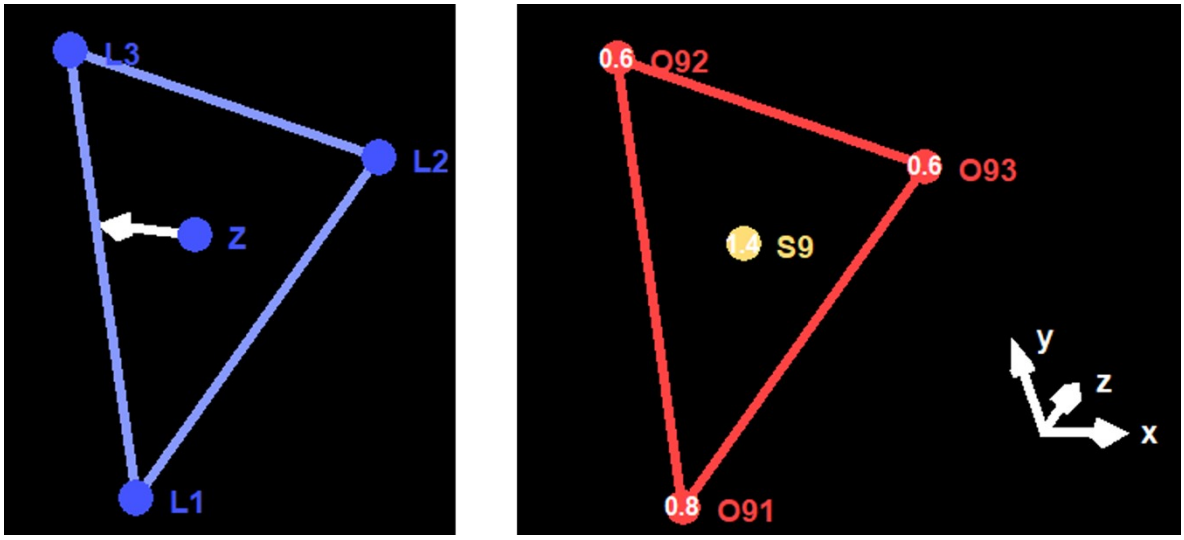

Figure S15: Geometric model (left) and fitted SO_3 unit (right) within the Polynator software. The white numbers within the right picture are the deviations of the atomic positions from the ideal positions in pm.

It should be noted that the δ value of the reference is not zero, since even a perfect trigonal planar arrangement would only lead to a perfect triangular arrangement if all atoms are completely within one plane. This is usually not the case within any matrix that allows atomic interaction, i.e. solution and solid phase. Nonetheless, the very small δ value of 0.752 shows that there is a nearly perfect trigonal planar geometry for the free SO_3 unit. Nonetheless, the interaction of the central sulfur atom with the adjacent Lewis bases (LB), i.e. the polysulfate chains, is strong enough to cause a slight distortion, although being at least 283 pm apart.

All relevant data is summarized in table S 33. Since the number of published tetrasulfates is very small we used reported group I, II, as well as ammonium penta- and hexasulfates for further comparison. We also added the data of the compounds $Te[S_2O_7]_2$, $[ReO_2Cl][S_2O_7]$ and the Dioxane·SO_3 mono- and diadduct as examples for extremely strongly coordinating cations and molecular species with O–donor atoms.

Table S35: Summarized bond lengths, δ values and CCDC/CSD numbers for the analyzed compounds.

LB-S bond length [pm]	Delta (triangle) [δ]	CCDC/CSD	Compound / Reference	Legend
157.6	14.868	425326	$Te[S_2O_7]_2$ [22]	$Te[S_2O_7]_2$
160.1	14.643	425326	$Te[S_2O_7]_2$ [22]	$Te[S_2O_7]_2$
162.2	13.37	419178	$[ReO_2Cl][S_2O_7]$ [23]	$[ReO_2Cl][S_2O_7]$
163.7	13.179	419178	$[ReO_2Cl][S_2O_7]$ [23]	$[ReO_2Cl][S_2O_7]$
163.3	13.092	2405912	$[ICl_2]_2[S_2O_7]$ [*this work*]	Interhalogen (I-centered)
164.5	12.829	425326	$Te[S_2O_7]_2$ [22]	$Te[S_2O_7]_2$
164	12.571	2405912	$[ICl_2]_2[S_2O_7]$ [*this work*]	Interhalogen (I-centered)
166.5	12.194	425326	$Te[S_2O_7]_2$ [22]	$Te[S_2O_7]_2$
164	12.12	2405909	$[ICl_2][HS_2O_7]$ [*this work*]	Interhalogen (I-centered)
171.3	10.962	2405908	$[IBr_2]_2[S_4O_{13}]$ [*this work*]	Interhalogen (I-centered)
170.5	10.928	2405908	$[IBr_2]_2[S_4O_{13}]$ [*this work*]	Interhalogen (I-centered)
170.7	10.873	426689	$Ca[S_3O_{10}]$ [24]	Group 2
169.4	10.767	423476	$Pb[S_3O_{10}]$ [25]	$Pb[S_3O_{10}]$
169.9	10.668	426689	$Ca[S_3O_{10}]$ [24]	Group 2
171.2	10.524	2405913	$[I_3]_4[S_4O_{13}]_2 \cdot SO_3$ [*this work*]	Interhalogen (I-centered)
172.3	10.499	2405913	$[I_3]_4[S_4O_{13}]_2 \cdot SO_3$ [*this work*]	Interhalogen (I-centered)
174	10.181	2405913	$[I_3]_4[S_4O_{13}]_2 \cdot SO_3$ [*this work*]	Interhalogen (I-centered)
175.52	9.974	428770	$Rb_2[S_6O_{19}]$ [26]	Group 1
174.7	9.887	2405913	$[I_3]_4[S_4O_{13}]_2 \cdot SO_3$ [*this work*]	Interhalogen (I-centered)
175.3	9.846	2405910	$Li_2[S_4O_{13}]$ [*this work*]	Group 1
177.5	9.828	1955943	$I_4[S_6O_{19}]$ [2]	$I_4[S_6O_{19}]$
176.5	9.565	2405910	$Li_2[S_4O_{13}]$ [*this work*]	Group 1
177.3	9.276	431359	$Li_2[S_5O_{16}]$ [27]	Group 1
178.7	9.201	426688	$Ba[S_4O_{13}]$ [24]	Group 2
180.6	9.094	431351	$Ag_2[S_5O_{16}]$ [27]	$Ag_2[S_5O_{16}]$
182.5	8.829	431363	$Na_2[S_5O_{16}]$ [27]	Group 1
188.7	7.513	261233	Dioxane · SO_3 [28]	Dioxane adducts
190.1	7.454	428769	$Cs_2[S_5O_{16}]$ [27]	Group 1
191.13	7.358	431221	$NH_4[S_6O_{19}]$ [26]	$NH_4[S_6O_{19}]$
192.1	7.254	261234	Dioxane · $2SO_3$ [28]	Dioxane adducts
193.3	6.923	261234	Dioxane · $2SO_3$ [28]	Dioxane adducts
196.19	6.625	428770	$Rb_2[S_6O_{19}]$ [26]	Group 1
195.9	6.53	428769	$Cs_2[S_5O_{16}]$ [27]	Group 1
230.9	2.905	431221	$NH_4[S_6O_{19}]$ [26]	$NH_4[S_6O_{19}]$
283.6	0.752	2405913	$[I_3]_4[S_4O_{13}]_2 \cdot SO_3$ [*this work*]	Interhalogen (I-centered)

For polysulfates, the Lewis base is the bridging oxygen atom between the terminal SO_3 unit and the first inner-lying sulfate unit of the chain. Thus, upon chain growth, i.e. the coordination and subsequent covalent linkage of another SO_3 unit by a former terminal oxygen atom, a geometric transition from the trigonal planar geometry of the uncoordinated SO_3 unit towards a tetrahedral coordinated SO_4 unit takes place.

Increasing the *Lewis* basicity of the oxoanion or increasing the Lewis acidity of the sulfur atom at the SO_3 unit will lead to a stronger O–SO_3 bond and an increased δ-value, respectively. The Lewis acidity of the sulfur atom cannot be influenced as this would require substitution of the oxygen atoms. However, a weakly bonded terminal SO_3 unit will become increasingly stable if it acts as a *Lewis* base itself and coordinates towards a stronger Lewis acidic centre compared to SO_3. This trend is shown by the increasing δ-value when comparing the group I penta- and hexasulfates, i.e. higher δ-values for harder cations (Li > Na > Cs > Rb). Even if for these structures pure electrostatic interactions are assumed, the trend is also visible for the herein presented structures containing triatomic group VII cations.

It is noteworthy that, in terms of coordination chemistry, the polysulfate chain length of our so far isolated species decreased with increasing Lewis acidity of the stabilized cation ($[ICl_2]^+$ > $[IBr_2]^+$ > $[I_3]^+$ > $[I_4]^{2+}$]. If the coordination is sufficiently strong, i.e. the oxoanionic position is blocked, no further polysulfate chain growth will occur. This means, stronger Lewis acidic cations will suppress the polysulfate chain growth. This might be an explanation for the so far elusive $[IF_2]^+$ compound, regardless of the weakly coordinating anions used.

E. Computational Details

All density functional theory (DFT) calculations were performed using the TURBOMOLE 7.7 program package [29] and the X-ray coordinates. The PBE0 hybrid functional [30] with the D4 dispersion correction [31] was employed, in conjunction with the def2-TZVP basis set.[32] For iodine atoms, effective core potentials (ECPs) including scalar relativistic effects were utilized to account for relativistic contributions.[33]

To analyze the nature of noncovalent interactions, the quantum theory of atoms in molecules (QTAIM) analysis [34] was performed using the Multiwfn program.[35] The topological parameters, including bond critical points (BCPs) and electron density values, were extracted to characterize halogen and chalcogen bonding interactions.

Natural Bond Orbital (NBO) analysis [36] was conducted using the NBO 7.0 program [37] to investigate orbital donor-acceptor interactions and quantify stabilization energies associated with LP(O) → σ*(I–X) charge transfer. The second-order perturbation energies provided insights into the electronic contributions to halogen bonding interactions.

All calculations were performed in the gas phase to isolate intrinsic electronic effects and avoid solvent-induced perturbations. The electrostatic potential (ESP) surfaces were computed to visualize σ-hole and π-hole distributions, providing further validation of the directional nature of the interactions.

For the IR calculations we used clusters extracted from the solid state ensuring the neutrality of the assemblies at the BP86[38, 39]-D4/def2-TZVP level of theory and the TURBOMOLE 7.7 program package. See below for the cartesian coordinates.

F. Cartesian Coordinates

Table S 36: Cartesian Coordinates for the IR calculations.

$[IBr_2]_2[S_4O_{13}]$					$[I_3]_4[S_4O_{13}]_2(SO_3)$			
I	-1.487897	3.389568	0.015144		I	1.083032	-1.290609	-4.49385
Br	-0.796518	5.385947	1.274897		I	3.062195	-0.868078	-2.736095
Br	-3.815049	3.246748	0.969614		I	-0.27722	-3.113859	-3.058208
I	1.487895	-3.389541	-0.015069		I	-2.609153	4.184774	-2.918195
Br	0.796517	-5.38592	-1.274821		I	-0.530955	4.587722	-1.272274
Br	3.815083	-3.246754	-0.969671		I	-4.233756	2.839496	-1.26642
I	-8.890973	0.000111	0.712232		I	2.255712	-3.930917	2.651227
Br	-6.747828	0.365721	-0.500848		I	3.66405	-2.17057	1.165444
Br	-9.878674	-1.728653	-0.739481		I	0.268838	-4.334196	0.909157
I	8.891007	-0.000117	-0.712289		I	-0.686144	0.768134	4.69945
Br	6.747779	-0.365735	0.500846		I	0.855689	2.223397	3.05822
Br	9.878624	1.728639	0.739479		I	-3.053299	0.738223	3.404025
S	1.275329	3.338664	-2.455096		S	6.220161	-0.255966	-0.756383
S	2.538044	0.866747	-1.52097		S	5.555842	2.020317	0.927062
S	2.401644	1.794556	1.19298		S	3.208915	2.622302	-0.627631
S	3.24927	-0.78093	2.162169		S	2.6004	4.913414	1.049953
O	2.600772	2.299506	-2.142285		O	7.035705	-0.918628	0.210794
O	0.990776	3.910548	-1.162634		O	4.815059	-0.572981	-0.669604
O	0.227407	2.488305	-2.937544		O	6.722643	-0.114631	-2.084744
O	1.90423	4.196595	-3.404442		O	5.726995	1.196224	2.060501
O	1.739249	1.130002	-0.1414		O	5.904425	3.399446	0.90558
O	3.868359	0.500673	-1.229506		O	1.871733	2.196752	-0.473653
O	1.670076	0.018681	-2.24231		O	3.957672	2.41275	-1.836008
O	3.531155	0.783792	1.547871		O	2.803342	3.993484	2.13666
O	1.34649	1.743605	2.117379		O	1.216609	5.069394	0.611974
O	3.039133	2.987514	0.831163		O	3.39294	6.096627	1.084858
O	2.945423	-0.558617	3.54896		O	6.239072	1.401895	-0.327057
O	4.51658	-1.374512	1.896771		O	3.982695	1.871625	0.59298
O	2.136251	-1.255881	1.378201		O	3.372274	4.141169	-0.283472
S	-1.275378	-3.338678	2.455094		S	-2.795228	-4.989386	-1.278264
S	-2.538009	-0.866753	1.520913		S	-3.898473	-3.437582	0.941603
S	-2.401693	-1.79457	-1.192983		S	-4.201198	-1.182573	-0.784457
S	-3.249236	0.780924	-2.162227		S	-5.909059	0.405311	0.933037
O	-2.600774	-2.29948	2.142361		O	-1.383667	-5.048757	-1.561836
O	-0.990825	-3.910562	1.162631		O	-3.381995	-6.179919	-0.750239
O	-0.227408	-2.488279	2.93762		O	-3.564263	-4.224587	-2.233581
O	-1.904231	-4.196568	3.404517		O	-3.387015	-2.55013	1.900088
O	-1.739298	-1.130016	0.141397		O	-4.7799	-4.480517	1.267957
O	-3.868325	-0.500679	1.229449		O	-2.80756	-1.263863	-1.013419
O	-1.670042	-0.018688	2.242252		O	-5.125188	-0.905584	-1.805127
O	-3.53112	-0.783798	-1.547929		O	-5.488591	0.932358	2.187859
O	-1.346409	-1.743571	-2.117358		O	-6.751564	-0.747791	0.958307
O	-3.039183	-2.987528	-0.831165		O	-6.210942	1.36727	-0.096227
O	-2.945313	0.55856	-3.548909		O	-2.68598	-3.939249	0.104784
O	-4.516629	1.374498	-1.896773		O	-4.728705	-2.579173	-0.172157
O	-2.136217	1.255875	-1.378258		O	-4.357082	-0.214031	0.421427
					S	-0.532152	0.374749	-0.584045
					O	0.206841	-0.689658	-0.029737
					O	-0.499232	0.621585	-1.9553
					O	-1.263032	1.2157	0.262712

References

1. G. Brauer, *Handbuch der Präparativen Anorganischen Chemie*, F. Enke, Stuttgart, 3 edn., 1975.
2. D. van Gerven, S. Sutorius, J. Bruns and M. S. Wickleder, *ChemistryOpen*, 2022, **11**, e202200122.
3. R. J. Gillespie and K. Malhotra, *Inorg. Chem.*, 1969, **8**, 1751-1756.
4. R. J. Gillespie and M. J. Morton, *Q. Rev. Chem. Soc.*, 1971, **25**, 553-570.
5. T. Birchall and R. D. Myers, *Inorg. Chem.*, 1981, **20**, 2207-2211.
6. R. A. M. Chand Paul, C. L. Arora and K. C. Malhotra, *J. Inorg. Nucl. Chem.*, 1971, **33**, 991-995.
7. Bruker AXS, *APEX 5 v2023.9-2*, 2023, Madsion, Winconsin, USA.
8. Bruker AXS, *Saint V8.40B*, 2012, Madsion, Winconsin, USA.
9. L. Krause, R. Herbst-Irmer, G. M. Sheldrick and D. Stalke, *J. Appl. Crystallogr.*, 2015, **48**, 3-10.
10. O. V. Dolomanov, L. J. Bourhis, R. J. Gildea, J. A. K. Howard and H. Puschmann, *J. Appl. Crystallogr.*, 2009, **42**, 339-341.
11. G. Sheldrick, *Acta Crystallogr. Sect. A*, 2015, **71**, 3-8.
12. G. Sheldrick, *Acta Crystallogr. Sect. C*, 2015, **71**, 3-8.
13. Crystal Impact GbR, *Diamond 4.6.8*, 2022, Bonn, Germany.
14. Bruker Optik GmbH, *OPUS 6.5*, 2009, Deutschland.
15. OriginLab Corporation, *OriginPro, Version 2024*, 2024, Northampton, MA, USA.
16. Renishaw plc., *WiRE 5.1*, 2017, New Mills, UK.
17. W. Wilson and F. Aubke, *Inorg. Chem.*, 1974, **13**, 326-332.
18. T. Birchall and R. D. Myers, *Inorg. Chem.*, 1983, **22**, 1751-1756.
19. J. Li, S. Irle and W. E. Schwarz, *Inorg. Chem.*, 1996, **35**, 100-109.
20. C. Logemann, T. Klüner and M. S. Wickleder, *Angew. Chem. Int. Ed.*, 2012, **51**, 4997-5000.
21. L. Link and R. Niewa, *J. Appl. Crystallogr.*, 2023, **56**, 1855-1864.
22. C. Logemann, J. Bruns, L. V. Schindler, V. Zimmermann and M. S. Wickleder, *Z. Anorg. Allg. Chem.*, 2015, **641**, 831-837.
23. U. Betke, W. Dononelli, T. Klüner and M. S. Wickleder, *Angew. Chem. Int. Ed.*, 2011, **50**, 12361-12363.
24. J. Bruns, C. Kolb and M. S. Wickleder, *Z. Anorg. Allg. Chem.*, 2014, **640**, 2345.
25. C. Logemann and Mathias S. Wickleder, *Z. Anorg. Allg. Chem.*, 2010, **636**, 2075-2075.
26. L. V. Schindler and M. S. Wickleder, Göttingen, 2015.
27. L. V. Schindler, M. Struckmann, A. Becker and M. S. Wickleder, *Eur. J. Inorg. Chem.*, 2017, **2017**, 958-964.
28. L. Richtera, J. Taraba and J. Toužín, *Collect. Czech. Chem. Commun.*, 2006, **71**, 155-163.
29. S. G. Balasubramani, G. P. Chen, S. Coriani, M. Diedenhofen, M. S. Frank, Y. J. Franzke, F. Furche, R. Grotjahn, M. E. Harding, C. Hättig, A. Hellweg, B. Helmich-Paris, C. Holzer, U. Huniar, M. Kaupp, A. Marefat Khah, S. Karbalaei Khani, T. Müller, F. Mack, B. D. Nguyen, S. M. Parker, E. Perlt, D. Rappoport, K. Reiter, S. Roy, M. Rückert, G. Schmitz, M. Sierka, E. Tapavicza, D. P. Tew, C. van Wüllen, V. K. Voora, F. Weigend, A. Wodyński and J. M. Yu, *J. Chem. Phys.*, 2020, **152**.
30. C. Adamo and V. Barone, *J. Chem. Phys.*, 1999, **110**, 6158-6170.
31. S. Grimme, S. Ehrlich and L. Goerigk, *J. Comput. Chem.*, 2011, **32**, 1456-1465.
32. F. Weigend and R. Ahlrichs, *Phys. Chem. Chem. Phys.*, 2005, **7**, 3297-3305.
33. K. A. Peterson, D. Figgen, M. Dolg and H. Stoll, *J. Chem. Phys.*, 2007, **126**.
34. R. F. W. Bader, *Acc. Chem. Res.*, 1985, **18**, 9-15.
35. T. Lu and F. Chen, *J. Comput. Chem.*, 2012, **33**, 580-592.
36. A. E. Reed, R. B. Weinstock and F. Weinhold, *J. Chem. Phys.*, 1985, **83**, 735-746.
37. E. D. Glendening, C. R. Landis and F. Weinhold, *J. Comput. Chem.*, 2019, **40**, 2234-2241.
38. A. D. Becke, *Phys. Rev. A*, 1988, **38**, 3098-3100.
39. J. P. Perdew, *Phys. Rev. B*, 1986, **33**, 8822-8824.